ANNUAL REVIEWS

Annual Review of Vision Science

Morphology, Molecular Characterization, and Connections of Ganglion Cells in Primate Retina

Ulrike Grünert[1,2] and Paul R. Martin[1,2]

[1]Save Sight Institute, Faculty of Medicine and Health, The University of Sydney, Sydney NSW 2000, Australia; email: ulrike.grunert@sydney.edu.au, paul.martin@sydney.edu.au

[2]Sydney Node, Australian Research Council Centre of Excellence for Integrative Brain Function, The University of Sydney, Sydney NSW 2000, Australia

Annu. Rev. Vis. Sci. 2021. 7:73–103

The *Annual Review of Vision Science* is online at vision.annualreviews.org

https://doi.org/10.1146/annurev-vision-100419-115801

Keywords

primate retina, ganglion cell types, parallel pathways, vision

Abstract

The eye sends information about the visual world to the brain on over 20 parallel signal pathways, each specialized to signal features such as spectral reflection (color), edges, and motion of objects in the environment. Each pathway is formed by the axons of a separate type of retinal output neuron (retinal ganglion cell). In this review, we summarize what is known about the excitatory retinal inputs, brain targets, and gene expression patterns of ganglion cells in humans and nonhuman primates. We describe how most ganglion cell types receive their input from only one or two of the 11 types of cone bipolar cell and project selectively to only one or two target regions in the brain. We also highlight how genetic methods are providing tools to characterize ganglion cells and establish cross-species homologies.

1. INTRODUCTION

1.1. Background

Different visual modalities such as color and motion are processed in parallel within the retina and then sent to higher brain regions via different types of retinal ganglion cells (Wässle 2004). Ganglion cells receive visual information from photoreceptors via bipolar and amacrine cells (**Figure 1*a***) and transmit these signals via the optic nerve to different visual centers of the brain. Ganglion cells vary with respect to their morphology, retinal connectivity, central projections, and response properties. Traditionally, they have been subdivided based on the morphology and size of their dendritic tree. For example, the best-studied ganglion cell types in the primate retina, midget and parasol cells (**Figure 1*b,c***), differ in the size of their dendritic trees, with midget cells having consistently smaller dendritic trees than parasol cells throughout the retina. Recent studies have begun to distinguish retinal ganglion cells in human and nonhuman primate retina by combining molecular methods and histological methods such as single-cell RNA sequencing, viral transduction, biolistic transfection, fluorescence in situ hybridization, and immunohistochemistry (Cowan et al. 2020, Hoshino et al. 2017, Jüttner et al. 2019, Peng et al. 2019, Yan et al. 2020). These advances herald the dawn of a new era for retinal neuroscience, that is, molecular-assisted comparative retinal anatomy.

1.2. Scope of This Review

We review recent advances in understanding the intraretinal connections and central projections of primate ganglion cells, together with their more recently revealed molecular characteristics. The physiological properties of primate ganglion cells have been the subjects of comprehensive reviews (Crook et al. 2014b, Field & Chichilnisky 2007, Kling et al. 2019, Lee et al. 2010), and readers are referred to these reviews for details of physiology.

The macaque retina is the traditional model experimental system for primate vision, and physiological and anatomical studies of this model use a variety of techniques ranging from retrograde labeling (Dacey et al. 2003, Leventhal et al. 1981, Rodieck & Watanabe 1993), to intracellular recordings in vivo (Lee et al. 1989) and in vitro (Dacey & Lee 1994, Dacey et al. 2005, Manookin

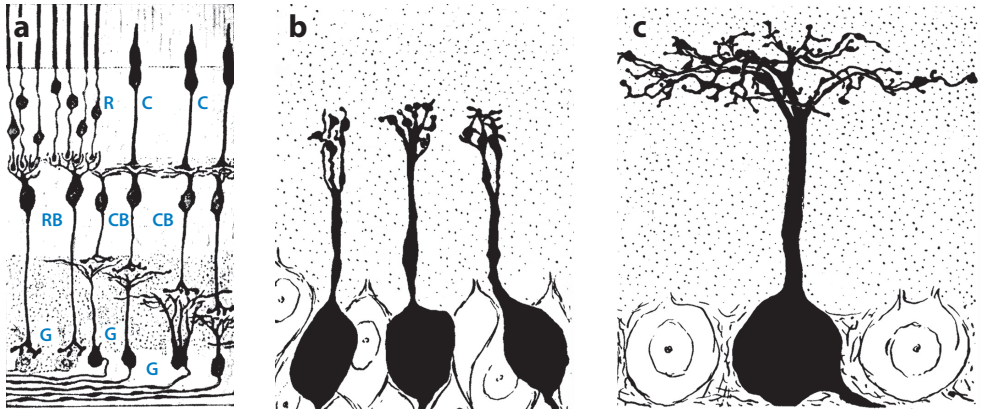

Figure 1

Vertical view of the retina. (*a*) Signal flow in the mammalian retina drawn by Ramón y Cajal in 1901 (public domain). Rods (R) contact rod bipolar cells (RB), and cones (C) contact cone bipolar cells (CB). Cone bipolar cells contact ganglion cells (G) at different levels of the inner plexiform layer. (*b,c*) Drawings of Golgi-impregnated (*b*) midget and (*c*) parasol ganglion cells from the central retina in the macaque. Panels *b* and *c* adapted with permission from Polyak (1941).

et al. 2018, Puller et al. 2015), to in vitro array recordings (Chichilnisky & Baylor 1999, Field et al. 2010, Li et al. 2015), to in vivo imaging (Gray et al. 2008; McGregor et al. 2020; Yin et al. 2011, 2014). Some of these methods are now being applied to the human retina (Cowan et al. 2020, Jüttner et al. 2019, Liu et al. 2017). Much of what we describe in this review is thus naturally based on studies in the macaque, but we also consider recent results from the human and marmoset retina.

2. TOPOGRAPHY OF RETINAL GANGLION CELLS IN PRIMATES

2.1. Comparison to Other Mammals

Diurnal (day-active) primates have the largest number of retinal ganglion cells of all mammals. For example, rabbits have a total of approximately 400,000, and cats have approximately 150,000 to 200,000 ganglion cells, but macaque monkeys have between 1 and 1.5 million ganglion cells (for a review, see Masri et al. 2019). Primates also achieve the highest densities of ganglion cells; for example, macaques have a peak density of approximately 50,000 ganglion cells per mm^2, whereas the peak density of ganglion cells in the cat (Wässle et al. 1981), rabbit (Vaney 1980), and mouse (Jeon et al. 1998) is around or below 10,000 cells per mm^2. The high number of ganglion cells in diurnal primates is due to the presence of a macula, where ganglion cell bodies occur up to eight layers deep (**Figure 2*a***). Thus, in foveate primates such as humans, an area of approximately 7% of the retina contains approximately 50% of the ganglion cells (Curcio & Allen 1990).

2.2. Primate Macular Topography and Comparison to Mice

Comparison of macular topography in three diurnal primates, humans (**Figure 2*b***), macaques (**Figure 2*c***), and marmosets (**Figure 2*d***), shows that the similarities outweigh the differences. The peak cone density at the fovea lies between 200,000 (human) and 300,000 (marmoset) cells/mm^2. Ganglion cells connecting to foveal cones via bipolar cells are shifted up to 0.4 mm away from the cone outer segments by cone Henle fibers and oblique processes of bipolar cells. Furthermore, as noted above, in the macula, the ganglion cells are stacked up to eight layers deep. Thus, although peak ganglion cell density is lower than peak cone density, the retinal volume in which these ganglion cells are contained is much larger (roughly proportional to the square of distance from the fovea). The upshot of all of this is that, within the central-most 1–2 mm, the number of ganglion cells is easily more than double the number of cones that feed them (Masri et al. 2020, Schein 1988, Wässle et al. 1989, Wilder et al. 1996).

The divergent pattern of macular connectivity is common to the three primate species shown in **Figure 2**. For example, within 170 μm (radius) of the center of the fovea, almost 9,000 cones are connected to 21,000 ganglion cells that are located up to 620 μm eccentricity in human retina (ratio 2.3 ganglion cells/cone; **Figure 2*b***), and the studies cited above have estimated ganglion cell–to-cone ratios between 2 and 4 for all three species. By contrast, there is numerical convergence from cones to ganglion cells throughout the mouse retina (average ganglion cell–to-cone ratio of 0.6; **Figure 2*e***), and a fovea-sized region of the mouse retina would house fewer than 1,000 ganglion cells. The foveal specializations in diurnal primates support high behavioral acuity (30–60 cycles/deg) compared to the modest behavioral acuity of mice (0.5 cycles/deg). Mice, on the scale of human visual performance, are legally (but not totally) blind.

2.3. Diversity of Primate Ganglion Cells

To date, at least 17 morphological (Dacey 2004, Dacey et al. 2003, Kolb et al. 1992, Masri et al. 2019, Yamada et al. 2005) and molecular (Peng et al. 2019) types of ganglion cells have been

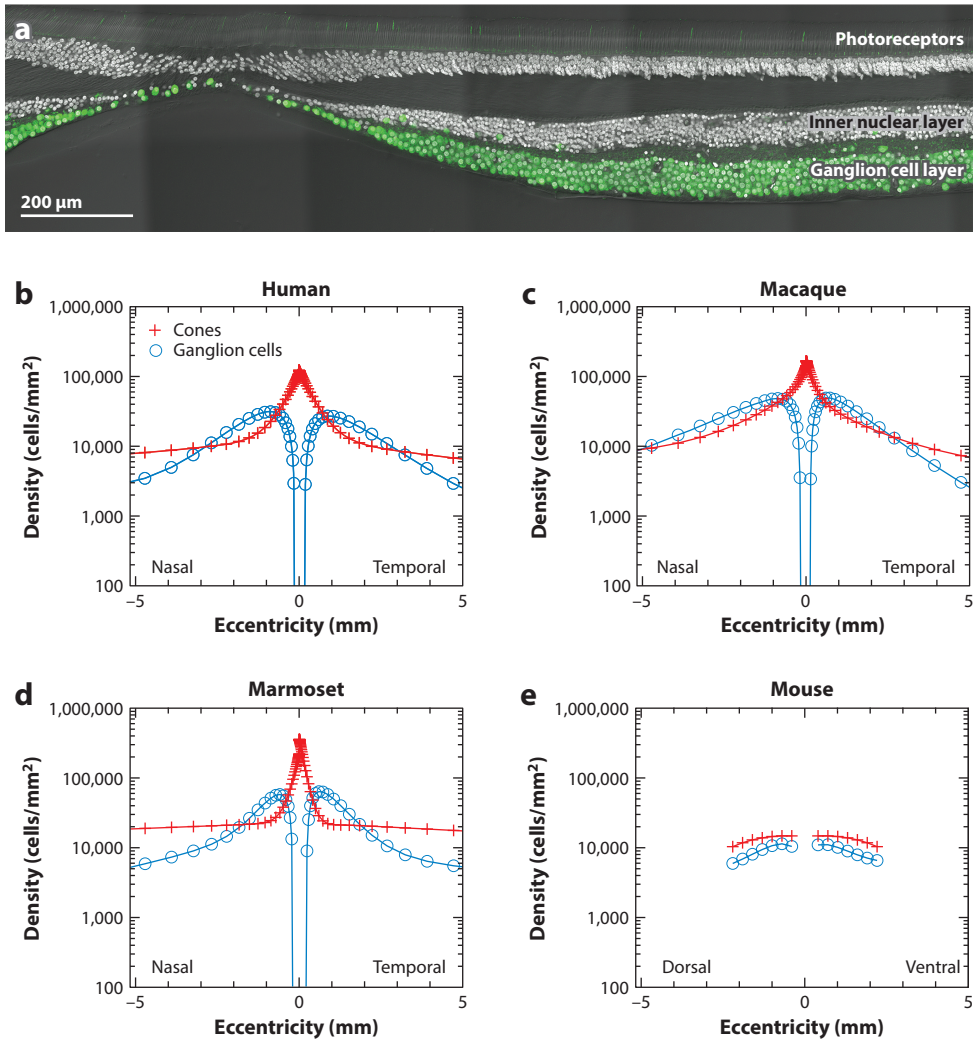

Figure 2

Spatial densities of ganglion cells. (*a*) Confocal image of a vertical section through the human fovea (Masri et al. 2020). Ganglion cells show RBPMS immunolabeling (*green*); other cell bodies are labeled with DAPI (*white*). (*b–d*) Spatial density of cone photoreceptors and ganglion cells in the central-most five millimeters of the (*b*) human, (*c*) macaque monkey, and (*d*) marmoset monkey retina. Data are plotted relative to the cone peak density. Note that ganglion cells are displaced by up to 400 µm from the cone photoreceptors by Henle fibers and oblique bipolar cell processes. Data in panel *b* taken from Curcio & Allen (1990) and Curcio et al. (1990). Data in panel *d* taken from Wilder et al. (1996). (*e*) Spatial density of cone photoreceptors and ganglion cells across the entire (approximately 5 mm diameter) mouse retina. Data are plotted relative to the position of the optic disk. Data taken from Jeon et al. (1998).

distinguished in the primate retina. The morphology of these ganglion cell types is comparable in Old World primates such as humans and macaques, and similar ganglion cell types have been found in diurnal New World primate species such as marmosets and capuchin monkeys (Ghosh et al. 1996, Ivanova et al. 2010, Moritoh et al. 2013, Silveira et al. 2004, Yamada et al. 1998).

Some species-related differences, however, have been found on the molecular level (**Table 1**). As detailed below (Section 2.4), the best-understood types are the three so-called classical ganglion cell types (midget, parasol, and small bistratified), with more recently studied nonclassical or wide-field types making up the remainder.

2.4. Distribution of Classical and Nonclassical Ganglion Cell Types

There is good agreement among studies that, in the fovea, midget cells make up 80–90% of the ganglion cells, and parasol cells make up 5–10% (Dacey 1993b, Grünert et al. 1993, Masri et al. 2019, Perry et al. 1984, Silveira & Perry 1991). Midget cells also form the majority of ganglion cells in the peripheral retina, but their proportion drops to approximately 50% (Crook et al. 2014b, Masri et al. 2019). Data from two recent molecular analyses estimated an over 70% proportion of midget cells in the peripheral retina of macaques (Peng et al. 2019) and humans (Yan et al. 2020).

Non-midget, non-parasol ganglion cell types likely make a small contribution to the fovea (Calkins & Sterling 2007, Calkins et al. 1998, Percival et al. 2013) and a more significant contribution to the peripheral retina (Dacey 2004, Masri et al. 2019). One of these is the now well-characterized small bistratified (SBS) ganglion cell type (see Section 4.3), which is estimated to make up approximately 6% of the ganglion cell population in the peripheral retina. The remaining nonclassical ganglion cells are low-density ganglion cell types and are also referred to as wide-field ganglion cells because they have relatively large dendritic fields compared to midget, parasol, and SBS cells.

3. STRATIFICATION IN THE INNER PLEXIFORM LAYER

In primates, there are 11 types of cone bipolar cells that contact cones and one type of rod bipolar cell that contacts rods (Boycott & Wässle 1991; Joo et al. 2011; Tsukamoto & Omi 2015, 2016) (**Figure 3*a*,*b***). The axons of different bipolar types terminate in different strata of the inner plexiform layer (IPL), where they make synaptic connections with ganglion and amacrine cells. Bipolar cells are customarily divided into ON types (which are depolarized at light onset) and OFF types (which are depolarized at light offset) (for a review, see Grünert & Martin 2020). There are five types of OFF cone bipolar (**Figure 3*a***), six types of ON cone bipolar, and one type of ON rod bipolar cell (**Figure 3*b***). The axons of OFF bipolar cells terminate in the outer half of the IPL, and the axons of ON bipolar cells terminate in its inner half (**Figure 3*a*,*b***). The axonal stratification of specific bipolar cell types has also been measured using immunohistochemical markers in macaque and marmoset retinas (Jusuf et al. 2004, Percival et al. 2013, Weltzien et al. 2015) (**Figure 3*c*–*h***) and is summarized in a schematic diagram in **Figure 4**. The IPL can be subdivided into five strata of equal thickness, named S1–S5. The outer strata (0–46% depth) contain the axon terminals of the OFF diffuse bipolar (DB) types DB1–DB3 and flat midget bipolar cells, as well as the processes of OFF starburst amacrine cells. The inner strata (48–100%) contain the ON bipolar types DB4–DB6, giant bipolar, invaginating midget bipolar, and rod bipolar cells as well as the processes of the ON starburst amacrine cells. The middle of the IPL is dominated by the processes of wide-field amacrine cells, whereas narrow-field amacrine cells are found throughout the entire IPL (for a review, see Grünert & Martin 2020). Amacrine cells usually provide the major synaptic input to all of the retinal ganglion cells that have been studied to date, but the functional roles of most amacrine cells remain to be determined. In this review, we focus on the ganglion connectivity with cone bipolar cells; the amacrine connectivity has been covered in another recent review (Grünert & Martin 2020). For our present purposes, the starburst amacrine cells, which can be identified with

Table 1 Summary of ganglion cell types in the primate retina

Morphological type	Physiological type	Bipolar input[a]	Percentage of total ganglion cells in the peripheral retina of the macaque[b]	Central projection (species)	Molecular marker (species)
Midget (inner)	Sustained ON; red–green opponent	IMB (Calkins et al. 1994, Kolb & DeKorver 1991, Tsukamoto & Omi 2016, Wool et al. 2019)	48%	LGN, parvocellular (macaque, marmoset) (Dacey et al. 2003; Jusuf et al. 2006a,b; Leventhal et al. 1981; Perry et al. 1984; Szmajda et al. 2008)	TPBG (macaque, human) (Peng et al. 2019, Yan et al. 2020); RBPMS2 (human) (Yan et al. 2020); EOMES (macaque, marmoset) (Peng et al. 2019)
Midget (outer)	Sustained OFF; red–green opponent	FMB (Calkins et al. 1994, Kolb et al. 1991, Wool et al. 2019)			TBR1 (macaque) (Peng et al. 2019); RBPMS2 (human) (Yan et al. 2020); Meis2 (macaque, human, and marmoset fovea) (Peng et al. 2019)
Parasol (inner)	Transient ON; achromatic	DB4, DB5, IMB (Girresch 2020, Puthussery et al. 2013, Tsukamoto et al. 2016)	15%	LGN, magnocellular, SC (macaque, marmoset) (Crook et al. 2008b, Dacey et al. 2003, Kwan et al. 2019, Leventhal et al. 1981, Perry et al. 1984, Szmajda et al. 2008)	CHRNA2 (macaque, human) (Peng et al. 2019, Yan et al. 2020); SPP1 (macaque, marmoset) (Peng et al. 2019); RBPMS2 (macaque) (Peng et al. 2019)
Parasol (outer)	Transient OFF; achromatic	DB2, DB3a (Calkins & Sterling 2007, Jacoby & Marshak 2000, Jacoby et al. 2000, Masri et al. 2016)			CA8 (macaque); SPP1 (macaque, marmoset) (Peng et al. 2019); FABP4 (human) (Yan et al. 2020); RBPMS2 (macaque) (Peng et al. 2019)
Small bistratified	Sustained ON; blue-ON/yellow-OFF	BB, DB2, DB3a (Calkins et al. 1998, Wool et al. 2019)	6%	LGN, koniocellular (macaque, marmoset) (Dacey et al. 2003, Percival et al. 2009, Rodieck 1991, Szmajda et al. 2008)	Calretinin (human) (Lee et al. 2016)
Large bistratified [S-group]	Blue-ON/yellow-OFF	DB2*, DB6*, BB*	3%	LGN, koniocellular, SC (macaque, marmoset) (Dacey et al. 2003, Percival et al. 2013, Rodieck 1991, Szmajda et al. 2008)	Calretinin (human) (Lee et al. 2016); Satb2
Smooth monostratified (inner)	Transient ON; achromatic	DB4, DB5 (Girresch 2020)	3%	LGN, SC (macaque, marmoset) (Crook et al. 2008a, Grünert et al. 2020)	Not known
Smooth monostratified (outer)	Transient OFF; achromatic	DB2*, DB3b*, DB3a (Masri et al. 2016)			Not known

(*Continued*)

Table 1 (*Continued*)

Morphological type	Physiological type	Bipolar input[a]	Percentage of total ganglion cells in the peripheral retina of the macaque[b]	Central projection (species)	Molecular marker (species)
Giant sparse (inner), melanopsin-expressing	Intrinsic photosensitive; blue-OFF/yellow-ON	BB (Patterson et al. 2020c); DB6 (Grünert et al. 2011, Liao et al. 2016)	1%	Pretectum, SCN, LGN, SC (macaque, human, marmoset) (Dacey et al. 2003, 2005; Grünert et al. 2011; Hannibal et al. 2004, 2014; Rodieck & Watanabe 1993; Szmajda et al. 2008)	OPN4 (melanopsin: macaque, human, marmoset) (Dacey et al. 2005, Hannibal et al. 2014, Jusuf et al. 2007, Liao et al. 2016, Nasir-Ahmad et al. 2019, Peng et al. 2019); PACAP (human, macaque) (Hannibal et al. 2004, 2014); calbindin (human) (Chandra et al. 2019)
Giant sparse (outer), melanopsin-expressing	Intrinsic photosensitive; blue-OFF/yellow-ON	DB1*, DB6 (Grünert et al. 2011, Liao et al. 2016)			
Large sparse (inner)	Blue-OFF/yellow-ON	BB*, DB6 (Percival et al. 2011)	2%	Pretectum, LGN (macaque, marmoset) (Dacey et al. 2003, Grünert et al. 2020, Percival et al. 2011, Rodieck & Watanabe 1993, Szmajda et al. 2008)	Satb2 (macaque) (Nasir-Ahmad et al. 2021)
Large sparse (outer)	Unknown	DB2*, DB3b*			Satb2 (macaque) (Dhande et al. 2019, Nasir-Ahmad et al. 2021)
Broad thorny [T-group]	Transient ON/OFF	DB2*, DB3a*, DB3b*, DB4*, GB*, DB5*	1.5%	LGN, SC (macaque, marmoset) (Dacey et al. 2003, Grünert et al. 2020, Percival et al. 2011, Rodieck & Watanabe 1993, Szmajda et al. 2008); inferior pulvinar (marmoset) (Kwan et al. 2019)	Calretinin (marmoset) (Chandra et al. 2017); Satb2 (marmoset) (Nasir-Ahmad et al. 2021)
Narrow thorny (inner)	Unknown	DB6 (Percival et al. 2014)	3%	LGN, SC (macaque, marmoset) (Dacey et al. 2003, Grünert et al. 2020, Percival et al. 2011, Rodieck & Watanabe 1993, Szmajda et al. 2008); inferior pulvinar (marmoset) (Kwan et al. 2019)	Calretinin (marmoset) (Chandra et al. 2017)
Narrow thorny (outer)	Unknown	DB2*			Calretinin (marmoset) (Chandra et al. 2017); Satb2 (marmoset) Nasir-Ahmad et al. 2021
Recursive bistratified [T-group]	ON–OFF direction selective?	DB2*, DB5*, GB*	1.5%	SC (Dacey 2004, Rodieck & Watanabe 1993); LGN?	Satb1 and Satb2 (marmoset) (Lee et al. 2019, Nasir-Ahmad et al. 2021)
Recursive monostratified [S-group]	ON direction selective?	?	4.5% (three mosaics?)	SC (Dacey 2004, Rodieck & Watanabe 1993); accessory optic system?	Not known

[a] Potential inputs based on costratification are marked with an asterisk.

[b] Data taken from Crook et al. (2014b).

Abbreviations: DB, diffuse bipolar; FMB, flat midget bipolar; IMB, invaginating midge bipolar; LGN, lateral geniculate nucleus; SC, superior colliculus; SCN, suprachiasmatic nucleus.

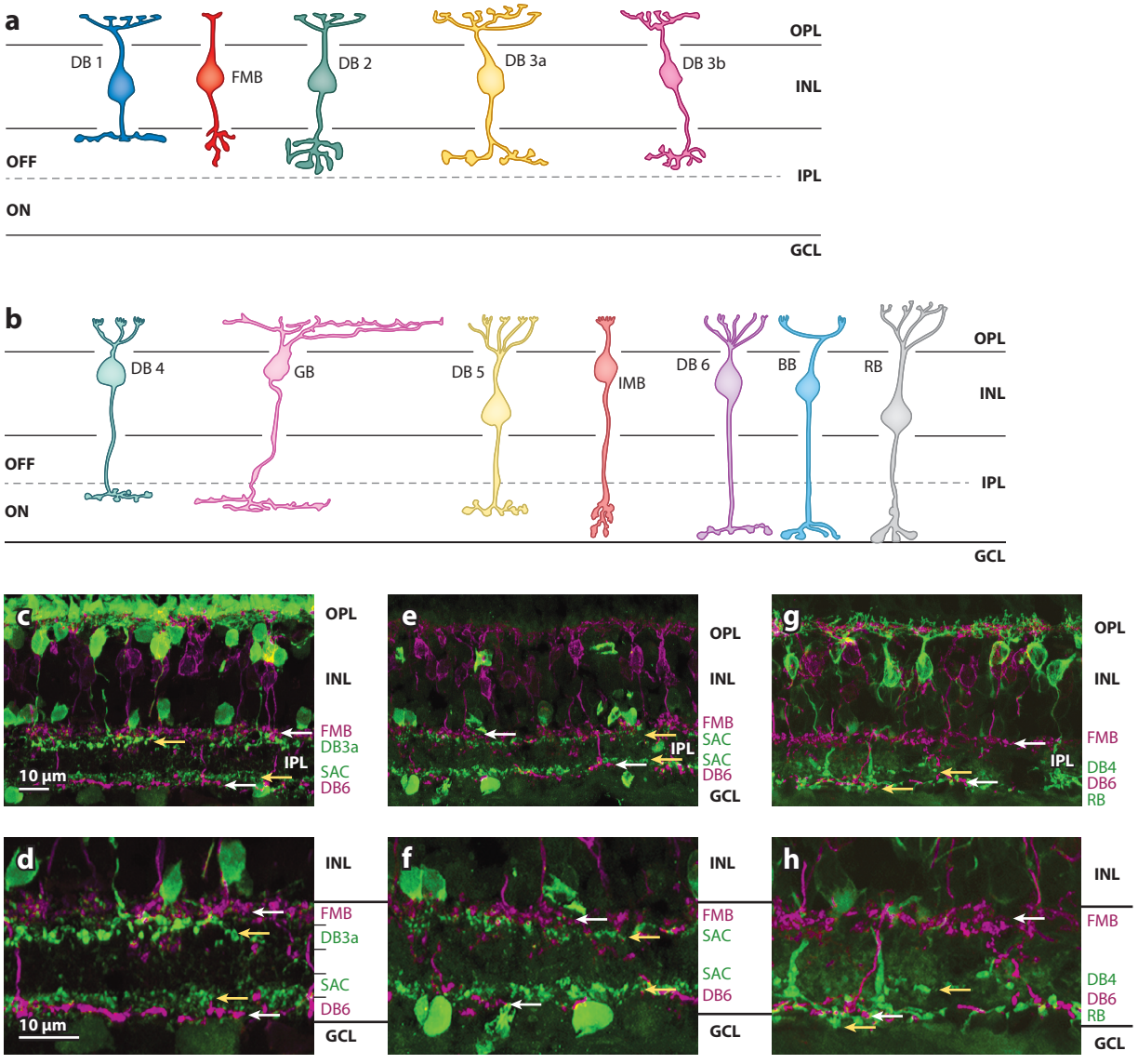

Figure 3

Bipolar types in the primate retina. (*a*,*b*) Schematic diagrams of the bipolar types in the primate retina. (*a*) OFF bipolar types. (*b*) ON bipolar types. Panels *a* and *b* adapted with permission from Boycott & Wässle (1991) and Grünert & Martin (2020). (*c*–*h*) Stratification in the IPL. Micrographs of immunolabeled vertical sections through the marmoset retina are shown. Antibodies against CD15 (*magenta*) label FMB and DB6 cells, which stratify in S1/2 and S5 (*white arrows*), respectively. (*c*,*d*) Antibodies against calbindin (*green*) label cone pedicles, DB3a cells (S2/3; *yellow arrow*), and a subpopulation of amacrine cells including inner starburst cells (SAC, S4; *yellow arrow*). (*e*, *f*) Antibodies against ChAT (*green*) identify inner and outer starburst cells (S2/3 and S4/5; *yellow arrows*). (*g*,*h*) Antibodies against PKCα (*green*) label rod bipolar and DB4 cells (*yellow arrows*) (for details, see Jusuf et al. 2004). Abbreviations: BB, blue cone bipolar; ChAT, choline acetyltransferase; DB, diffuse bipolar; FMB, flat midget bipolar; GB, giant bipolar; GCL, ganglion cell layer; IMB, invaginating midget bipolar; INL, inner nuclear layer; IPL, inner plexiform layer; PKCα, protein kinase Cα; OPL, outer plexiform layer; RB, rod bipolar.

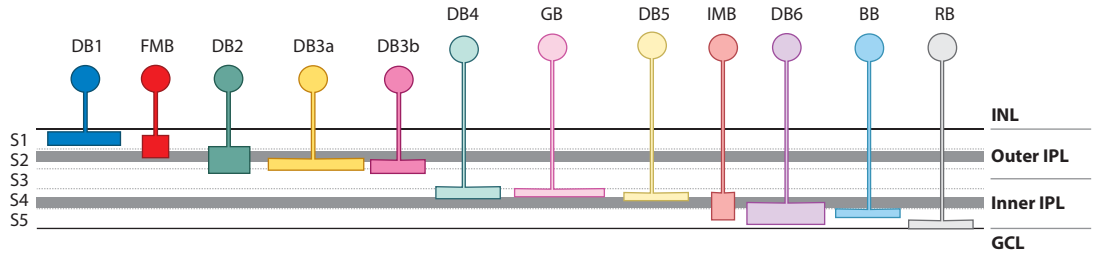

Figure 4

Schematic diagram of bipolar cell axonal stratification in the primate inner plexiform layer (IPL). The axon terminals of the bipolar types are shown together with the choline acetyltransferase (ChAT) bands (*gray*). The diffuse bipolar (DB) types DB1, DB2, DB3a, and DB3b and the flat midget bipolar (FMB) cell are OFF bipolar cells and stratify in the outer half of the IPL. The DB types DB4, DB5, and DB6; the giant bipolar (GB) cell; the blue cone bipolar (BB) cell; the invaginating midget bipolar (IMB) cell; and the rod bipolar (RB) cell are ON bipolar cells and stratify in the inner half of the IPL. The dendritic trees of the bipolar cells have been omitted. Note that ON bipolar somas tend to lie distal to OFF bipolar somas in the inner nuclear layer (INL).

antibodies, are important because their narrowly stratified processes act as guidelines in the IPL: ON starburst processes mark stratum S2, and OFF starburst processes mark stratum S4.

4. CLASSICAL GANGLION CELL TYPES

4.1. Midget Ganglion Cells

Midget ganglion cells, which derive their name from their small dendritic fields (Polyak 1941), are the most numerous ganglion cell type in the primate retina and are unique to primates. Midget ganglion cells are crucial for high-acuity and red–green color vision.

4.1.1. Morphology and connectivity with bipolar cells. Midget ganglion cells comprise inner (ON) and outer (OFF) stratifying cells. Foveal midget ganglion cells have very small, compact dendritic trees (**Figure 5*a***, *left*), whereas more peripheral midget ganglion cells have more diffuse dendritic trees (**Figure 5*a***, *right*). In the central retina, midget ganglion cells make

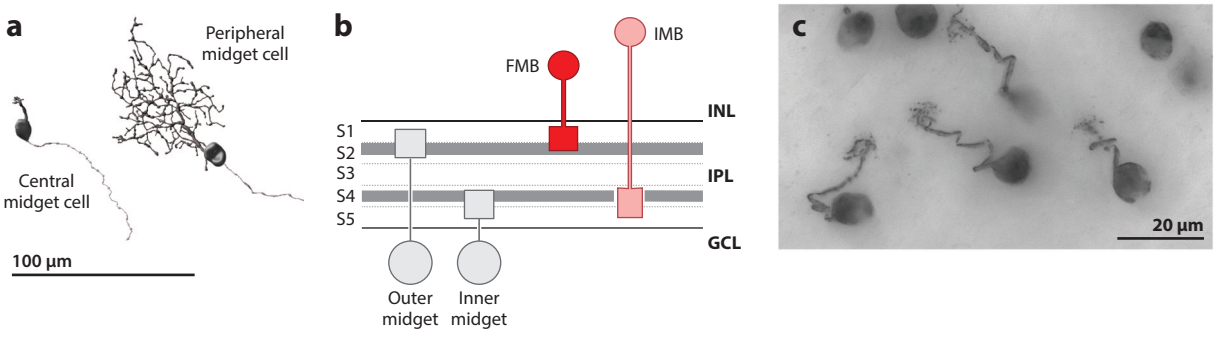

Figure 5

Midget ganglion cells. (*a*) Drawings of midget ganglion cells from the marmoset retina. The cell on the left is from the foveal retina. The cell on the right is from the peripheral retina (4.4 mm eccentricity). (*b*). The stratification of inner and outer midget cells is shown with respect to the ChAT bands (*gray*). The dominant input to outer midget cells derives from FMB cells, and the dominant input to inner midget cells derives from IMB cells. (*c*) Composite micrographs of midget ganglion cells from macaque fovea labeled following horseradish peroxidase injection into the optic tract (P.R. Martin, unpublished data). Abbreviations: ChAT, choline acetyltransferase; FMB, flat midget bipolar; GCL, ganglion cell layer; IMB, invaginating midget bipolar; INL, inner nuclear layer; IPL, inner plexiform layer; LGN, lateral geniculate nucleus.

one-to-one connections with OFF (flat) or ON (invaginating) midget bipolar cells (**Figure 5*b*,*c***), which in turn make one-to-one connections with cones. This connectivity, which is the basis for high-acuity vision and for red–green color vision, is present in Old World (Calkins et al. 1994, Kolb & DeKorver 1991) and New World primates (Chan et al. 2001, Jusuf et al. 2006b, Telkes et al. 2008) and emerges during fetal development by a process of refinement of initially less discriminate connections (Zhang et al. 2020). In the midperipheral retina, midget ganglion cells receive the large majority of their input from midget bipolar cells in both marmosets (Jusuf et al. 2006a) and macaques; Tsukamoto & Omi (2015, 2016) reported additional input from DB1 and DB6 cells to outer and inner cells, respectively.

In the macaque (but not the marmoset) retina, there is morphological and physiological evidence that, in the foveal region, approximately 5% of OFF midget ganglion cells receive input from short-wavelength-sensitive (S) cones via OFF midget bipolar cells (Klug et al. 2003, Patterson et al. 2019a, Tsukamoto & Omi 2015, Wool et al. 2019). In the peripheral retina of macaques and humans, midget bipolar cells receiving input from a single cone are found in up to about 40° of visual angle (Masri et al. 2020, Wässle et al. 1994), but at this eccentricity each midget ganglion cell receives input from multiple midget bipolar cells, resulting in nonselective input from all cone types, including S-cones (Diller et al. 2004, Field et al. 2010, Martin et al. 2001, Wool et al. 2019). Thus, in the peripheral retina, a pure blue-OFF midget ganglion cell type is not present (for a review, see Grünert & Martin 2020).

The connectivity in the midget pathway in the marmoset retina differs from that of macaques in that, in marmosets, single-cone-contacting midget bipolar cells are restricted to the fovea (Telkes et al. 2008). Thus, outside the fovea in marmosets, the medium-wavelength-sensitive (M)/long-wavelength-sensitive (L) cone input to midget ganglion cells is already mixed at the level of the cone contacts.

4.1.2. Percentage and molecular markers. As noted above, midget ganglion cells have been estimated to make up 80–90% of the ganglion cells in the fovea and approximately 50% of ganglion cells in the peripheral retina of macaques (Crook et al. 2014b, Dacey 2004); comparable values likely apply for humans (Dacey 1993b) and marmosets (Masri et al. 2019). Recent studies identified midget ganglion cells at the molecular level and also found genetic differences between inner and outer midget ganglion cells (Peng et al. 2019, Yan et al. 2020) (**Table 1**). These studies also showed that, in marmosets and humans, the somas of outer midget ganglion cells are located closer to the inner nuclear layer than those of inner midget ganglion cells.

4.1.3. Central projections and physiology. Retrograde labeling studies in macaques (Leventhal et al. 1981, Perry et al. 1984) and marmosets (Jusuf et al. 2006a, Szmajda et al. 2008) have demonstrated that the major input to the parvocellular layers of the dorsal lateral geniculate nucleus (LGN) derives from midget or (Pβ) ganglion cells. Moreover, there is good evidence that midget ganglion cells in both species do not target any other brain areas and thus project exclusively to the parvocellular layers of the LGN (Grünert et al. 2021, Kwan et al. 2019, Rodieck & Watanabe 1993).

Functional properties of midget-parvocellular cells have been discussed in recent reviews and thus are only briefly summarized in this article. Midget cells show sustained responses to maintained illumination and low and nonsaturating contrast sensitivity and have small receptive fields, consistent with a role in high-acuity vision at high image contrasts (for reviews, see Kling et al. 2019, Lee et al. 2010, Thoreson & Dacey 2019).

In and around the fovea, midget cells show red–green color opponent responses by virtue of low numerical convergence from M- and L-cone photoreceptors to the receptive field center and indiscriminate M/L inhibitory inputs to the surround (Wool et al. 2018; but see also Patterson

et al. 2019b). Red–green opponent responses deteriorate with greater convergence of M/L cone inputs at greater eccentricities, with only mild biases toward M- or L-cones in either the center or surround (Field et al. 2010, Wool et al. 2018).

Over the past decade, the properties of midget-parvocellular cell receptive fields recorded in whole-animal preparations with intact optics and the properties recorded in vitro from macaque retina have gradually converged. For example, foveal midget cells recorded in vivo from animals with intact optics show more sustained responses than their peripheral counterparts (Solomon et al. 2002), and in vitro measurements show only weak inhibitory inputs to foveal compared to peripheral midget cells (Crook et al. 2011, Sinha et al. 2017).

Four recent papers reported recordings of midget ganglion cells in in vitro preparations of human retina. Three of these studies (Cowan et al. 2020, Kling et al. 2020, Soto et al. 2020) found clear similarities in spatial and temporal properties of human midget receptive fields to previous studies of macaque and marmoset midget-parvocellular pathway fields (for reviews, see Kling et al. 2019, Lee et al. 2010, Thoreson & Dacey 2019). The fourth (Reinhard & Münch 2021) found relatively fewer examples of typical midget-parvocellular-type receptive fields and overall only mild functional distinctions among recorded receptive fields. Differences in tissue preservation quality, visual stimulus, and eccentricity of recorded cells could underlie this discrepancy.

4.2. Parasol Ganglion Cells

Parasol cells were named by Polyak (1941, p. 312) for their characteristic morphology (**Figure 1*c***), which "resembles somewhat an open Chinese umbrella or parasol." They make up the second largest population of ganglion cells in the primate retina and play a role in motion detection and acuity at low image contrasts.

4.2.1. Morphology and connectivity with bipolar cells. Parasol cells have thick primary dendrites that extend radially from a large soma (**Figure 6*a***). There are inner (ON) and outer (OFF) stratifying parasol cells, and their dendrites are located close to the center of the IPL (**Figure 6*b***) (Ghosh et al. 1996, Watanabe & Rodieck 1989). Parasol cells receive approximately 20% of their input from bipolar cells and approximately 80% from amacrine cells (Jacoby et al. 1996, Patterson et al. 2020a). The major bipolar input to outer parasol cells derives from DB3a cells (**Figure 6*c***) in macaque (Calkins & Sterling 2007, Jacoby & Marshak 2000, Jacoby et al. 2000, Tsukamoto & Omi 2015) and marmoset retinas (Masri et al. 2016, 2019). In addition, outer parasol cells receive some input from DB1, DB2, and DB3b cells (Tsukamoto & Omi 2015). The major bipolar input to inner parasol cells derives from DB4 cells, with additional input from DB5 cells and invaginating midget bipolar cells (Girresch 2020, Puthussery et al. 2013, Tsukamoto & Omi 2016).

4.2.2. Percentage and molecular markers. Retrograde labeling studies estimated that parasol (Pα) cells in macaques make up approximately 10% of the retinal ganglion cells in the peripheral retina (Perry et al. 1984). Similar proportions were obtained using neurofibrillar staining in macaques (Silveira & Perry 1991) and immunohistochemical staining in the New World monkey *Saimiri* (Hughes et al. 1989). In the central retina, immunohistochemical studies using antibodies against $GABA_A$ receptors in the macaque retina estimated that parasol cells make up between 5% and 8% of the ganglion cell population (Grünert et al. 1993). The mosaic properties of inner and outer parasol cells differ, with inner cell diameters in macaques being approximately 30% larger than those of their outer counterparts (Dacey & Petersen 1992), suggesting that outer cells occur at higher densities. According to recent estimates from molecular studies, the proportion of outer parasol cells is lower in the peripheral than in the foveal retina, but the proportion of inner parasol cells remains constant (Peng et al. 2019, Yan et al. 2020).

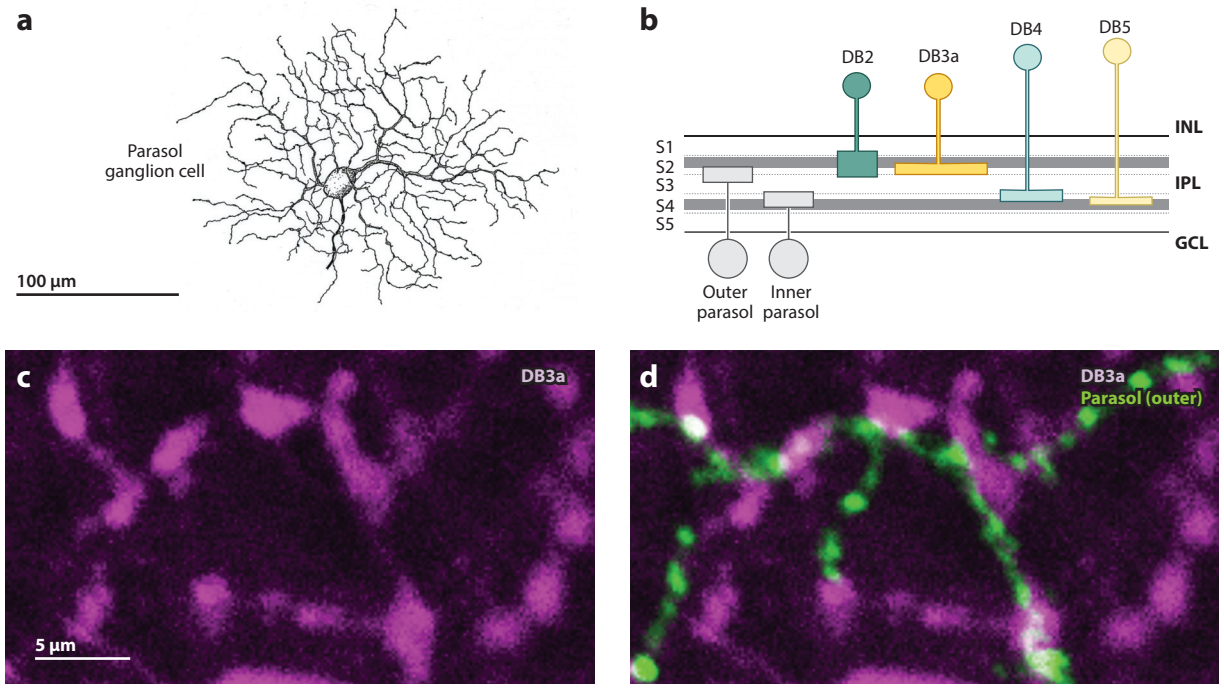

Figure 6

Parasol cells. (*a*) Drawing of an inner parasol ganglion cell from the marmoset retina. Drawing provided by K.K. Ghosh. Eccentricity is 6.5 mm. (*b*) The stratification of inner and outer parasol cells is shown with respect to the ChAT bands (*gray*). The dominant input to outer parasol cells derives from DB2 and DB3a cells, whereas inner parasol cells receive most of their input from DB4 and DB5 cells. Eccentricity is 4.0 mm. (*c*) Confocal image of calbindin-labeled DB3a axon terminals (*magenta*). (*d*) The image in panel *c* is shown together with the dendrites of an outer parasol cell (*green*). The processes of the two cells are closely associated. Abbreviations: ChAT, choline acetyltransferase; DB, diffuse bipolar; GCL, ganglion cell layer; INL, inner nuclear layer; IPL, inner plexiform layer.

In macaques, parasol cells have been suggested to be immunoreactive to antibodies against carbonic anhydrase (CA) 8 (Puthussery et al. 2013) and molecular studies found the CA8 gene in outer parasol cells of the macaque (Peng et al. 2019) but not of the human (Yan et al. 2020) retina. Other molecular markers for parasol cells are listed in **Table 1**.

4.2.3. Central projections and physiology. Parasol cells were originally suggested to project preferentially to the magnocellular layers of the LGN, with only a low number projecting to the superior colliculus (Leventhal et al. 1981, Perry & Cowey 1984, Perry et al. 1984, Rodieck & Watanabe 1993). More recently, however, it has been established for macaques (Crook et al. 2008b) and marmosets (Grünert et al. 2021, Kwan et al. 2019) that a substantial proportion of parasol cells projects to the superior colliculus. This projection is thought to derive from a branching axon, with the other branch going to the LGN (Crook et al. 2008b).

Parasol cells show high contrast sensitivity and vigorous, transient responses to rapidly flickering or moving stimuli. These response properties reflect their functional role of feeding cortical and subcortical pathways for motion detection (for reviews, see Crook et al. 2014b, Lee et al. 2010). As is the case with midget cells (see above), many results from recent in vitro recordings have confirmed and extended principles first established in whole-animal recordings with intact optics. It has been established that parasol cells show nonlinear (Y-like) spatial summation, albeit

less prominently than do Y/alpha cells in the cat retina, likely reflecting functional subunits corresponding to diffuse bipolar cell inputs (Crook et al. 2008b, 2014a). Recent measurements (Appleby & Manookin 2020, Manookin et al. 2018, Turner & Rieke 2016) have explored nonlinearities in parasol cell receptive fields and their manifestation in responses to looming and moving stimuli and stimuli with frequency spectra emulating natural scenes. The pictures emerging from these studies are more complex and nuanced than the simplistic summary introduced above that parasol cells feed motion-detection pathways. However, it could be argued that this summary is still the best that we have as our understanding of parasol cell function moves forward.

4.3. Small Bistratified Ganglion Cells

SBS ganglion cells are equivalent to Polyak's shrub cells (see Dacey 1993a). They have dendritic field sizes comparable to those of parasol cells but show distinct morphology. SBS cells are involved in blue–yellow color vision (Dacey & Lee 1994).

4.3.1. Morphology and connectivity with bipolar cells. The morphology of SBS cells was first described in detail in macaque and human retinas (Dacey 1993a, Rodieck 1991), and cells with comparable morphology have subsequently been found in diurnal New World monkeys (Ghosh et al. 1996, Silveira et al. 1999). The dendritic field size of SBS cells is in the same range as that of parasol cells, but their morphologies are clearly different. SBS cells have a relatively sparse dendritic tree characterized by hooks and thorns (**Figure 7*a***). The inner dendritic tier is larger than the outer dendritic tier. The inner dendrites stratify in strata S4/S5, whereas the outer dendrites are located in S2 of the IPL (**Figure 7*b***). Intracellular recordings from SBS cells in the macaque retina showed that they have blue-ON and yellow-OFF responses (Crook et al. 2009, Dacey & Lee 1994). Electron microscopic studies confirmed that the inner dendritic tier of SBS cells receives input from blue cone bipolar cells (Calkins & Sterling 2007; Patterson et al. 2020b,c; Wool et al. 2019). The input to the outer tier has been suggested to include DB2 and DB3a cells (Calkins et al. 1998, Ghosh et al. 1997), but the proportions of input from the different types of bipolar cell to the outer ties are not known.

4.3.2. Percentage and molecular markers. Taking dendritic coverage and dendritic field area into account, the percentage of SBS cells in macaques increases from approximately 1.5% in the central retina to approximately 6% in the periphery, making it the third most common ganglion cell type in the primate retina (Dacey 1993a). In the human retina, cells with the morphology of SBS cells were found to be immunolabeled with antibodies against calretinin (Lee et al. 2016). In contrast, in the macaque retina, calretinin is not present in ganglion cells of adults (Hendrickson et al. 2007), and in the marmoset retina, calretinin is expressed by wide-field ganglion cell types (Chandra et al. 2017).

4.3.3. Central projections and physiology. In the macaque retina, SBS cells were identified after retrograde labeling from the LGN (Dacey et al. 2003, Rodieck 1991), and it was originally suggested that they project to the parvocellular layers. More recent tracer studies in marmosets found that SBS cells target the koniocellular layers of the LGN (Percival et al. 2009, Szmajda et al. 2008), which are located between the parvo- and magnocellular layers. The koniocellular layers are neurochemically distinct (Goodchild & Martin 1998, Hendry & Yoshioka 1994, Johnson & Casagrande 1995, Kaas et al. 1978). Consistently, electrophysiological recordings from the koniocellular layers in marmosets (Martin et al. 1997) and macaques (Roy et al. 2009) have demonstrated that cells with similar properties to SBS cells (named blue-ON cells) are segregated to the koniocellular layers.

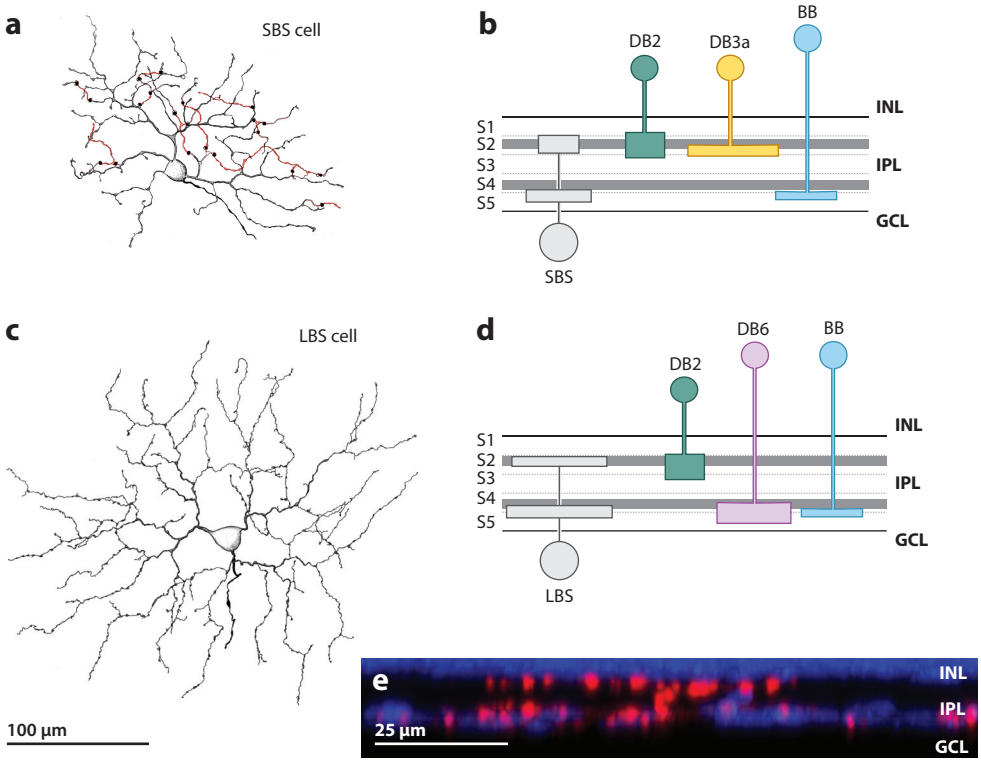

Figure 7

Small bistratified (SBS) and large bistratified (LBS) cells. (*a*) Drawing of an SBS cell in the marmoset retina obtained after intracellular injection. The inner dendrites are shown in black; the outer dendrites are shown in red. Drawing provided by K.K. Ghosh. Eccentricity is 4.4 mm. (*b*) Stratification and suggested connectivity. The inner dendrites of SBS cells receive input from blue cone bipolar cells, and the outer dendrites likely receive input from DB2 and DB3 cells. (*c*) Drawing of an LBS cell in the marmoset retina obtained after intracellular injection. Drawing provided by K.K. Ghosh. Eccentricity is 5.2 mm. (*d*) Stratification is shown with respect to the ChAT bands (*gray*) and suggested connectivity with diffuse bipolar cells. (*e*) Orthogonal view of a DiI-injected LBS cell together with DAPI-labeled (*blue*) cell nuclei in the INL and GCL. Additional abbreviations: ChAT, choline acetyltransferase; DB, diffuse bipolar; GCL, ganglion cell layer; INL, inner nuclear layer; IPL, inner plexiform layer.

Taken together, the current view is that SBS ganglion cells are part of the koniocellular pathway, which is considered to be evolutionarily older than the parasol-magnocellular and midget-parvocellular pathways (Jones 2001). However, in contrast to parasol cells and to wide-field ganglion cells, there is no evidence that SBS cells project to other subcortical visual centers (Dacey 2004, Grünert et al. 2021). The detailed physiological properties of SBS cells have been discussed in recent reviews (Crook et al. 2014b, Thoreson & Dacey 2019) and are not considered further in this article.

5. WIDE-FIELD GANGLION CELLS

5.1. Large Bistratified Cells

Large bistratified (LBS) cells have been observed in human, macaque, and marmoset retinas (Dacey 1993a, Dacey et al. 2003, Masri et al. 2019, Percival et al. 2013, Peterson & Dacey 2000,

Yamada et al. 2005). In macaque, LBS cells are part of the (collicular-projecting) S-group of cells (Rodieck & Watanabe 1993), and in the human retina, cells with a similar morphology were named G17 (Kolb et al. 1992, Lee et al. 2016). LBS cells resemble SBS cells in that they have relatively sparse dendritic trees (**Figure 7*c***) and stratify in similar regions of the IPL (**Figure 7*d***), but the dendritic field size of LBS cells is consistently larger than that of SBS cells at comparable eccentricities (Dacey 1993a, Dacey et al. 2003). Moreover, these studies found that SBS but not LBS cells are tracer coupled to amacrine cells.

Preliminary electrophysiological recordings from LBS cells in the macaque retina suggested that they have blue-ON and yellow-OFF responses (Dacey et al. 2003), but a full characterization of the response properties of LBS cells is still lacking. The synaptic connectivity of LBS cells has not been studied, but given their stratification and the evidence that they have blue-ON responses, the inner dendrites likely receive input from blue cone bipolar cells. The diffuse bipolar types DB2 and DB6 are additional candidates that may provide input to the inner dendrites, but this possibility needs to be supported by further studies. Although Masri et al. (2019) found some potential connections of LBS cells with DB3a cells in marmosets, it is unlikely that these cells provide significant input.

LBS cells are suggested to make up 3% of the ganglion cells in the peripheral retina of the macaque (Crook et al. 2014b). In marmosets, examples of LBS cells have also been found in the central retina (Percival et al. 2013), but their proportion has not been determined. In the human retina, LBS cells, like SBS cells, have been suggested to express the calcium-binding protein calretinin (Lee et al. 2016), and in macaques a bistratified cell type with similar morphology has been found to express the transcription factor Satb2 (Peng et al. 2019).

As noted above, there is evidence from retrograde tracer studies that LBS cells project to the superior colliculus (Rodieck & Watanabe 1993). Other studies detected LBS cells after tracer injections into the LGN (Dacey et al. 2003, Percival et al. 2013) and the pulvinar (Kwan et al. 2019).

5.2. Smooth Monostratified Cells

Smooth monostratified cells (referred to below as smooth cells) resemble parasol cells but have comparatively larger dendritic trees throughout the retina and have smaller soma and axon diameters. They have been studied in detail in the macaque retina (Crook et al. 2008a), and cells with similar morphology have also been found in human (Peterson & Dacey 1999) and marmoset retinas (Grünert et al. 2021, Masri et al. 2019).

5.2.1. Morphology and connectivity with bipolar cells. Smooth cells have relatively thick primary dendrites radiating from the soma (**Figure 8*a,c***). Analysis of the mosaic properties of smooth cells in the macaque showed that the somas are regularly spaced, and their dendritic trees tile the retina with minimal overlap, suggesting that they form independent spatial arrays (Crook et al. 2008a).

The dendrites of outer and inner stratifying smooth cells are found at the same level as those of outer and inner parasol cells, suggesting that they may share presynaptic partners. However, in marmosets, OFF smooth cells do not show the same strong connectivity to DB3a cells as has been shown for OFF parasol cells (Masri et al. 2016, 2019) (**Figures 5*c,d*** and **8*c,d***), suggesting that the weighting of the bipolar input differs between the two ganglion cell types. Based on their stratification, outer smooth cells may receive their major input from DB2 and DB3b cells. The input to inner smooth cells (**Figure 8*b***) has recently been found to derive predominantly from DB5 cells, with DB4 and giant bipolar cells also contributing (Girresch 2020).

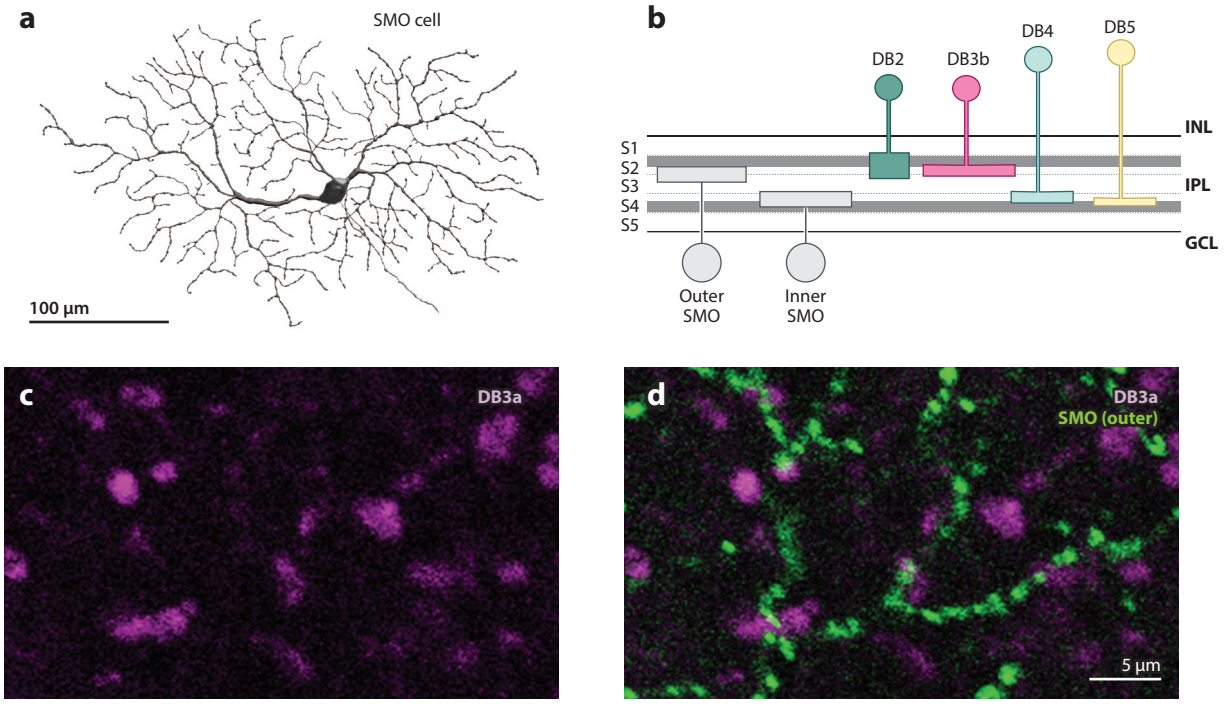

Figure 8

Smooth monostratified (SMO) cells. (*a*) Drawing of an outer SMO cell from the marmoset retina. The cell was obtained after retrograde labeling from the superior colliculus and intracellular injection (Grünert et al. 2021). Eccentricity is 6.4 mm. (*b*) Schematic diagram showing the stratification of inner and outer SMO cells with respect to the ChAT bands (*gray*) and suggested dominant presynaptic bipolar input. (*c*) Confocal image of calbindin-labeled DB3a axon terminals (*magenta*) (horizontal view). (*d*) The image in panel *c* is shown together with the dendrites of an outer SMO cell. DB3a axons have regions of overlap with SMO cells but are not closely associated (Masri et al. 2016, 2019). Additional abbreviations: ChAT, choline acetyltransferase; DB, diffuse bipolar; GCL, ganglion cell layer; INL, inner nuclear layer; IPL, inner plexiform layer.

5.2.2. Central projections and physiology. In macaque and marmoset retinas, smooth monostratified cells were identified after retrograde tracer injections into the superior colliculus and the LGN (Crook et al. 2008a, Grünert et al. 2021, Percival et al. 2013), but other retrograde labeling studies targeting the superior colliculus did not report these cells (Rodieck & Watanabe 1993). The specific layer(s) that these cells target in the superior colliculus and LGN have not been determined. Taking their mosaic properties into account (see above), it is likely that smooth cells project to both the superior colliculus and the LGN via branching axons.

Smooth cells show strong Y-like response signatures with frequency-doubled responses to counterphase gratings, consistent with the presence of rectifying receptive field subunits; have receptive fields 2–3 times the diameter of parasol cell fields at the same eccentricity; and show only weak signs of a receptive field surround (Crook et al. 2008a). Smooth cells likely correspond to the upsilon cells reported in array recordings, as their spatial and temporal response spectra show heavy overlap (Crook et al. 2008a, Petrusca et al. 2007). Their receptive field centers contain patches with high contrast sensitivity (Rhoades et al. 2019), but the size of the patches is unrelated to the local domains of bipolar axon terminals or the nonlinear subunit size (Crook et al. 2008a, Petrusca et al. 2007).

5.3. Giant Sparse (Melanopsin-Expressing) Cells

Intrinsically photosensitive ganglion cells containing the photopigment melanopsin are well characterized in the mouse retina, where they have been split into six types. In the mouse, each type shows a characteristic pattern of melanopsin expression, morphology, and functional and molecular properties (Do 2019). Similar diversity has been suggested for primate retina, but electrophysiological evidence to support such diversity is still emerging.

5.3.1. Morphology. Ganglion cells with very large, sparse dendritic trees have been observed in various primate retinas, including those of humans (Dacey et al. 2003, Kolb et al. 1992, Rodieck & Watanabe 1993, Yamada et al. 2005). These cells were named giant sparse cells and are now known to be equivalent to the intrinsically photosensitive melanopsin-expressing ganglion cells (Dacey et al. 2005). Because these cells can be immunohistochemically labeled, their distribution and morphology are well studied in macaque (Dacey et al. 2005, Liao et al. 2016), marmoset (Jusuf et al. 2007), and human (Hannibal et al. 2017, Liao et al. 2016, Nasir-Ahmad et al. 2019) retinas.

In primates, melanopsin-expressing cells comprise at least two types, an inner and an outer stratifying type (**Figure 9*a,b***). The outer stratifying cells strongly express melanopsin and make up the majority (approximately 60%) of the melanopsin-expressing cells. At least half of the outer stratifying cells have their soma displaced to the inner nuclear layer (INL outer cells); the remainder have their soma in the ganglion cell layer (GCL outer cells). The dendritic fields of the outer cells cover the retina independently of their soma location and thus are assumed from one type. The inner cells usually have weaker melanopsin expression, and their soma is located exclusively in the ganglion cell layer (GCL inner cells). Bistratified melanopsin-expressing cells have also been identified. These cells are comparatively rare, and they do not tile the retina. The majority of their dendrites are located close to the GCL, and their soma is located in the GCL. Thus, bistratified melanopsin-expressing cells are considered to be part of the inner stratifying population (Jusuf et al. 2007, Liao et al. 2016, Nasir-Ahmad et al. 2019).

A recent study in the human retina distinguished outer cells further based on their soma and dendritic field size and named them M1 and gigantic M1 cells (Hannibal et al. 2017). Like the other outer stratifying cells, the gigantic M1 cells have their soma in either the INL or GCL, but their dendritic fields show a large degree of overlap with those of the other outer cells. The gigantic M1 cells were thus suggested to form independent mosaics, but their spatial distribution across the retina has not been studied.

The same study split the inner cells into two types based on soma size and slight differences in stratification and suggested that they are equivalent to the mouse M2 and M4 cells. However, it has not been determined whether the two types form independent populations and whether they are physiologically different, as has been reported for mouse M2 and M4 cells (Do 2019).

5.3.2. Connectivity with bipolar and amacrine cells. Melanopsin-expressing cells receive synaptic input from bipolar and amacrine cells (Grünert et al. 2011, Jusuf et al. 2007, Liao et al. 2016, Nasir-Ahmad et al. 2019). The bipolar input to the outer stratifying cells derives from DB6 cells via en passant synapses, whereas the inner stratifying cells receive DB6 input via their axon terminals (**Figure 9*c***). The DB6 input to inner stratifying cells in the marmoset retina was estimated to make up approximately 30% of the bipolar input to the inner melanopsin-expressing cells (Grünert et al. 2011). For the macaque parafoveal retina, a recent serial electron microscopic reconstruction study showed that blue cone bipolar cells provide the large majority of the bipolar input to a large sparsely branching inner stratifying cell type (presumed to be the inner stratifying melanopsin cell) (Patterson et al. 2020c). These latter findings suggest that the inner stratifying cells have blue ON responses, but physiological evidence is still lacking.

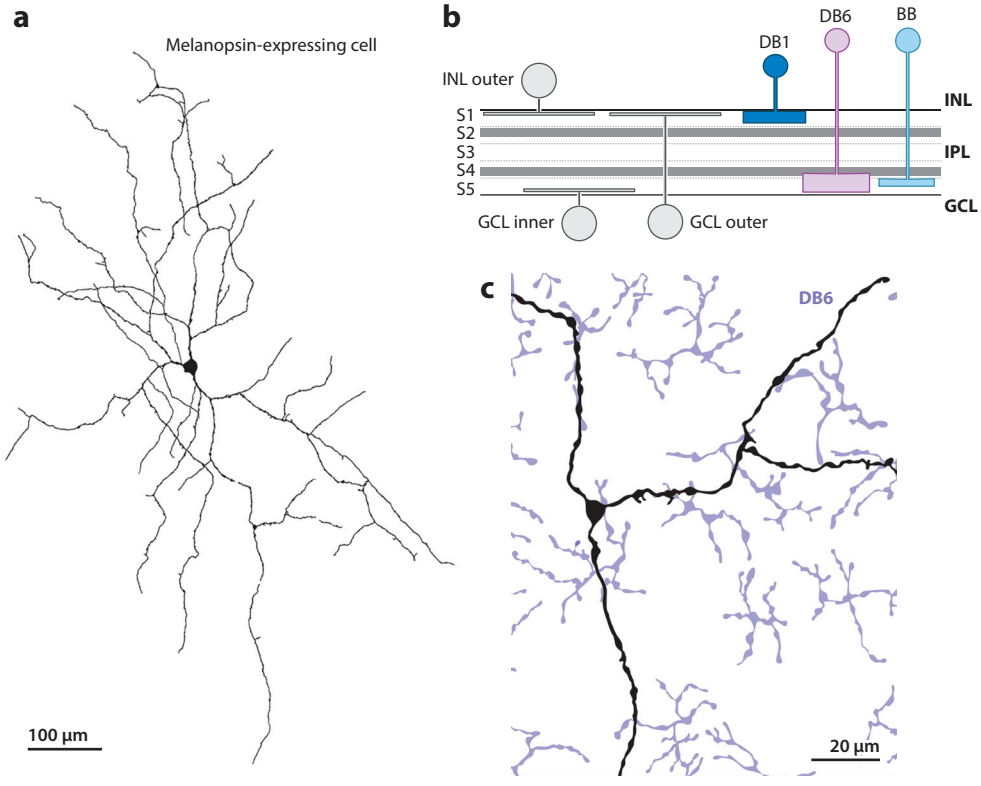

Figure 9

Giant sparse melanopsin-expressing cells. (*a*) Drawing of an inner stratifying melanopsin-expressing cell in the marmoset retina. Eccentricity is 4.9 mm. (*b*) Schematic diagram showing the stratification of inner and outer stratifying melanopsin-expressing cells with respect to the ChAT bands (*gray*). Outer stratifying melanopsin-expressing cells have their soma in either the INL (INL inner cells) or the GCL (GCL outer cells), whereas inner stratifying melanopsin-expressing cells have their soma in the GCL only (GCL inner cells). The bipolar cells suggested to provide input are shown. (*c*) Part of the dendritic tree of the cell shown in panel *a*, together with the overlaying DB6 axons. There are some potential points of contact between the two cell types (Grünert et al. 2011). Drawings in panels *a* and *c* provided by P.R. Jusuf. Abbreviations: ChAT, choline acetyltransferase; DB, diffuse bipolar; GCL, ganglion cell layer; INL, inner nuclear layer; IPL, inner plexiform layer.

A light microscopic study in the human retina suggested that both inner and outer melanopsin-expressing cells receive direct input from rod bipolar cells at their soma and proximal dendrites (Hannibal et al. 2017). Such direct input has not been found in the macaque or marmoset retinas (Grünert et al. 2011, Jusuf et al. 2007, Liao et al. 2016), but a recent electron microscopic study reported a single synapse between a rod bipolar axon and a presumed melanopsin-expressing cell in the macaque retina (Patterson et al. 2020b). Whether this connectivity is the anatomical substrate of the rod input to melanopsin-expressing cells found physiologically (Dacey et al. 2005) remains to be determined.

Patterson and colleagues (2020b) also showed that an amacrine cell type that receives selective input from blue cone bipolar cells makes synapses with the proximal dendrites of presumed GCL outer cells and suggested that the S-cone amacrine cell mediates the S-OFF response recorded in melanopsin cells (Dacey et al. 2005). These findings thus predict that the GCL outer cells differ

in their response characteristics from the INL outer cells, as the S-cone amacrine cell does not contact the dendrites of the INL outer cells.

5.3.3. Percentage and molecular markers. The total number of melanopsin-expressing cells was estimated to be approximately 3,000 cells in the macaque retina (Dacey et al. 2005) and 4,000–7,000 cells in the human retina (Hannibal et al. 2017, Liao et al. 2016), meaning that melanopsin-expressing cells in macaques would make up between 0.4% and 0.8% of the total ganglion cell population. These estimates are consistent with direct counts of melanopsin-expressing and total ganglion cell density in the human peripheral retina, where melanopsin-expressing cells make up 1% of the total population (Chandra et al. 2019). Melanopsin-expressing cells are present in the central retina, but their percentage there has not yet been determined. Interestingly, in the human retina, GCL inner cells appear to be nearly absent in the midperipheral temporal retina (Chandra et al. 2019, Hannibal et al. 2017, Nasir-Ahmad et al. 2019), but the significance of this uneven distribution remains unclear.

Although there are differences in the expression level of melanopsin between inner and outer cells (Hannibal et al. 2017, Nasir-Ahmad et al. 2019), different types of melanopsin-expressing cells have not yet been distinguished using other molecular markers in primate retina; however, at the genetic level, three clusters expressing melanopsin were distinguished in the macaque retina (Peng et al. 2019), and two clusters were distinguished in the human retina (Yan et al. 2020).

Apart from the expression of melanopsin, both inner and outer melanopsin-expressing cells in human and macaque retinas have been shown to express the neuropeptide pituitary adenylyl cyclase–activating polypeptide (Hannibal et al. 2004, 2014), which is essential for sustained pupil constriction (Keenan et al. 2016). Other studies found expression of calbindin in the inner and outer melanopsin-expressing cells of human but not marmoset retinas (Chandra et al. 2019).

5.3.4. Central projections and physiology. Retrograde tracer injections into different brain regions in macaques demonstrated that cells with the morphology of melanopsin-expressing cells (also named PT-sparse cells) project to the pretectum (Dacey et al. 2003, Rodieck & Watanabe 1993), the LGN (Dacey et al. 2005, Liao et al. 2016), the suprachiasmatic nucleus, and the superior colliculus (Hannibal et al. 2014). In primates, there is no evidence that different morphological types of melanopsin-expressing cells target different brain regions, as has been found for the mouse visual system (Do 2019).

Melanopsin-expressing ganglion cells contribute to both image-forming (color and pattern) vision and non-image-forming (sleep–wake cycles, mood regulation) vision in all mammalian species studied to date. The functional properties of their intrinsic melanopsin transduction pathway and photoreceptor inputs via bipolar and amacrine cells have been recently reviewed (Thoreson & Dacey 2019).

5.4. Large Sparse Cells

Large sparse cells are monostratified cells that have been identified in human (Kolb et al. 1992, Peterson & Dacey 1999), macaque (Dacey et al. 2003, Yamada et al. 2005), and marmoset retinas (Ghosh et al. 1996, Masri et al. 2019, Moritoh et al. 2013).

5.4.1. Morphology and connectivity with bipolar cells. Large sparse cells have sparse dendritic trees and stratify in either the OFF or the ON sublamina of the IPL close to its borders (**Figure 10**). Thus, they resemble giant sparse cells, but their dendritic field size is consistently smaller than that of giant sparse cells, and they do not express melanopsin (Dhande et al. 2019, Nasir-Ahmad et al. 2021).

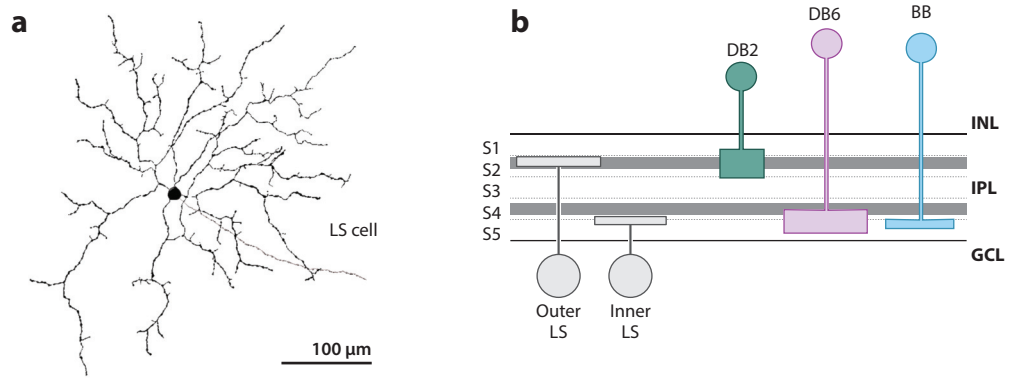

Figure 10

Large sparse (LS) cells. (*a*) Drawing of an inner stratifying LS cell in the marmoset retina. Eccentricity is 5.6 mm. (*b*) Schematic diagram showing the stratification of inner and outer stratifying LS cells with respect to the ChAT bands (*gray*), together with the potential bipolar input. Additional abbreviations: ChAT, choline acetyltransferase; DB, diffuse bipolar; GCL, ganglion cell layer; INL, inner nuclear layer; IPL, inner plexiform layer.

Light microscopy suggests that the bipolar input to inner stratifying sparse cells in the marmoset retina includes the diffuse bipolar type DB6 (Percival et al. 2011). The latter study found that most of the DB6 axon terminals lying within the dendritic field of a large sparse cell may provide input to that cell, but each DB6 axon terminal makes only very few putative contacts, suggesting that other ON bipolar types, e.g., blue cone bipolar cells, also provide input, as has been found for a similar ganglion cell type in the macaque retina (Patterson et al. 2020c).

5.4.2. Molecular markers. Large sparse cells in macaque and human (but not in marmoset) retinas were shown to express the transcription factor Satb2 (Dhande et al. 2019, Nasir-Ahmad et al. 2021). Thus, Satb2 cells in human and macaque retinas differ from those in mouse and rabbit retinas, where Satb2 was found to be a marker for direction-selective ganglion cells (Dhande et al. 2019, Sweeney et al. 2019), suggesting that transcription factor expression is not conserved within mammalian species.

5.4.3. Projections and physiology. Retrograde tracer experiments in macaques and marmosets suggest that large sparse cells project to the pretectum (Leventhal et al. 1981, Rodieck & Watanabe 1993), as well as to the LGN (Dacey et al. 2003, Percival et al. 2011, Szmajda et al. 2008). In marmosets, the koniocellular layers of the LGN (Percival et al. 2011, Szmajda et al. 2008), which house a relatively high proportion of blue-ON/yellow-OFF, as well as blue-OFF/yellow-ON cells, were identified as specific targets of large sparse cells (Szmajda et al. 2006), and in macaques, an inner large sparse cell recorded in vitro (Dacey 2004) showed blue-OFF/yellow-ON properties, but the physiological properties of outer large sparse cells are not known.

5.5. Broad Thorny Cells

Broad thorny cells [also named T-group cells by Rodieck & Watanabe (1993) and hedge cells by Ghosh et al. (1996)] are characterized by a dense dendritic tree decorated with fine thorns (**Figure 11*a***).

5.5.1. Morphology, connectivity with bipolar cells, and molecular markers. The dendrites of broad thorny cells occupy the middle of the IPL, sandwiched between the inner and outer

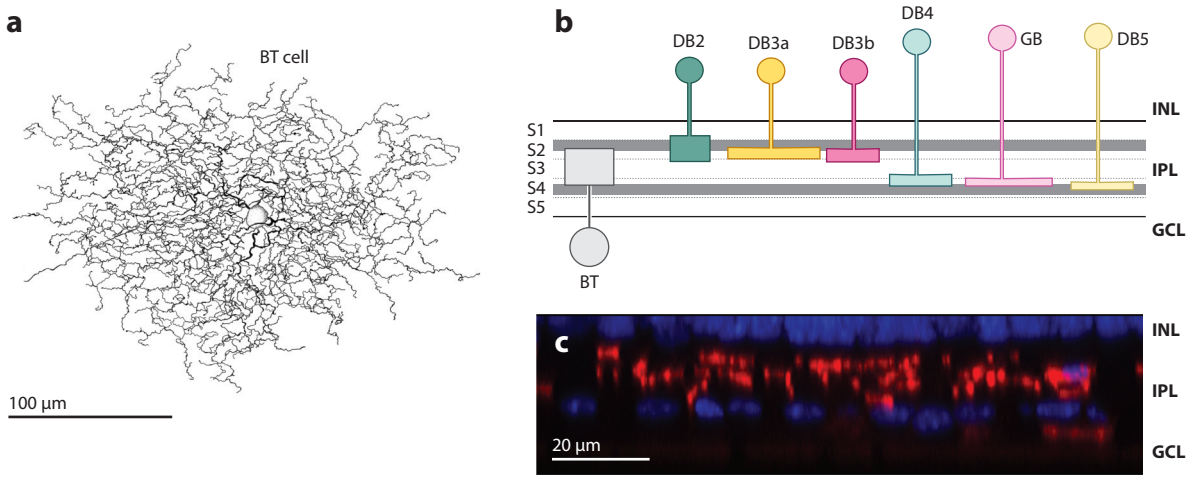

Figure 11

Broad thorny (BT) cells. (*a*) Drawing of a BT cell in the marmoset retina obtained after intracellular injections. Drawing provided by K.K. Ghosh. Eccentricity is 2.8 mm. (*b*) Schematic diagram showing the stratification of BT cells between the ChAT bands (*gray*) and the potential bipolar types providing input. (*c*) Orthogonal view of a DiI-injected BT cell (*red*) together with DAPI-labeled cell nuclei (*blue*) in the INL and GCL. Additional abbreviations: ChAT, choline acetyltransferase; DB, diffuse bipolar; GB, giant bipolar; GCL, ganglion cell layer; INL, inner nuclear layer; IPL, inner plexiform layer.

choline acetyltransferase (ChAT) bands (**Figure 11*b,c***). Thus, the dendrites of broad thorny cells could potentially make contact with multiple bipolar types, and light microscopic studies have consistently demonstrated that they receive bipolar input in the ON and OFF sublamina (Percival et al. 2011). A recent study of a foveal broad thorny cell in the macaque retina found that these cells receive input from ON and OFF bipolar cells, although the large majority of the input derived from amacrine cells (Bordt et al. 2021). The specific bipolar types providing the input have yet to be identified. In the marmoset but not in the macaque, broad thorny cells express the calcium binding protein calretinin (Chandra et al. 2017) and the transcription factor Satb2 (Nasir-Ahmad et al. 2021). The two populations do not overlap completely, suggesting that broad thorny cells may be subdivided based on their molecular properties.

5.5.2. Projections and physiology. In macaques and marmosets, broad thorny cells project to the superior colliculus (Kwan et al. 2019, Rodieck & Watanabe 1993) and the LGN (Dacey et al. 2003, Grünert et al. 2021, Percival et al. 2011, Szmajda et al. 2008); additionally, in marmosets, the koniocellular layers of the LGN were identified as the specific targets of these cells. However, in marmosets, broad thorny cells were only rarely encountered after LGN tracer injections (Percival et al. 2011, 2013; Szmajda et al. 2008) compared to the relatively high number obtained after biolistic labeling (Masri et al. 2019, Moritoh et al. 2013), viral labeling (Ivanova et al. 2010), and retrograde injections into the superior colliculus (Grünert et al. 2021, Kwan et al. 2019). Thus, it is likely that the superior colliculus is the major target of broad thorny cells.

The morphology of primate broad thorny cells resembles that of local edge detectors, which are the smallest and most common ganglion cell type in the rabbit retina (Rockhill et al. 2002, van Wyk et al. 2006). These cells respond to both light ON and light OFF, and electrophysiological recordings from broad thorny cells in the macaque retina showed some properties compatible with properties of local edge detectors in the rabbit retina (for example, strong surround suppression

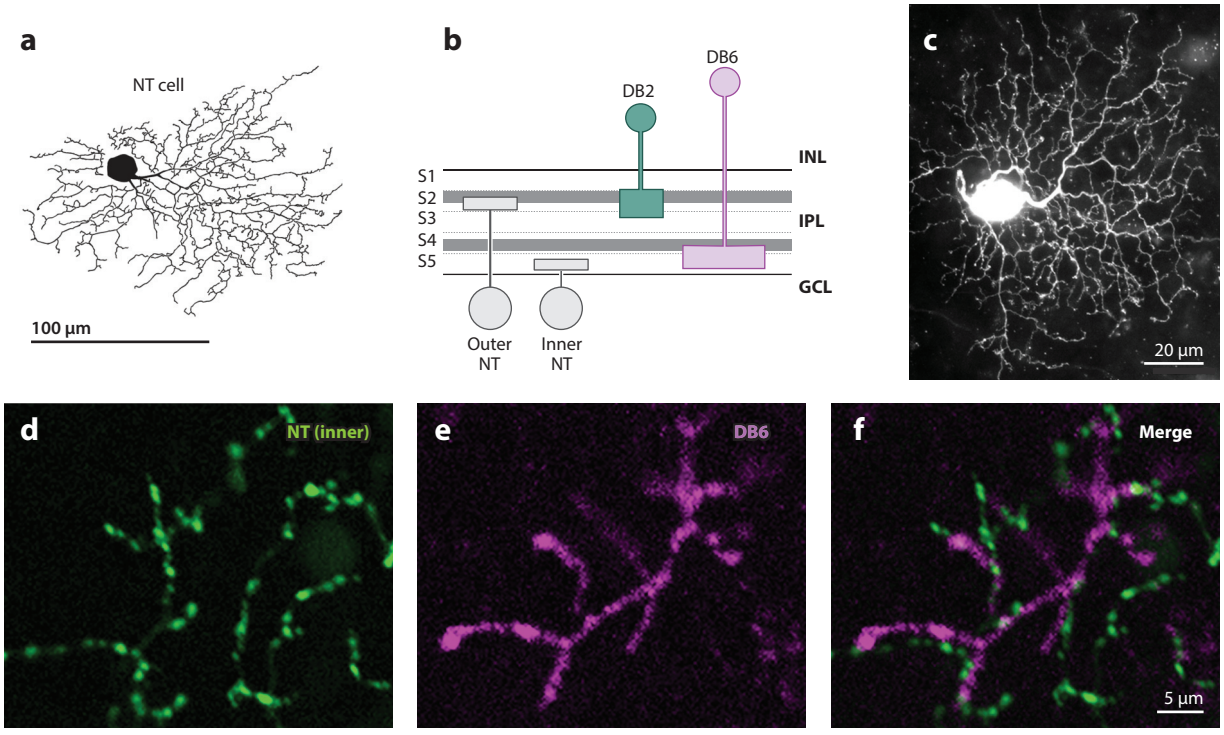

Figure 12

Narrow thorny (NT) cells. (*a*) Drawing of an inner stratifying NT cell in the marmoset retina obtained after retrograde labeling from koniocellular layer K1 of the LGN. Eccentricity is 4.5 mm. (*b*) Schematic diagram showing the stratification of inner and outer NT cells with respect to the ChAT bands (*gray*) and the suggested bipolar types providing input. (*c*) Micrograph of retrogradely labeled NT outer cells obtained after tracer injection into layer K1 of the LGN. Eccentricity is 3.6 mm. (*d*) Confocal image showing part of the dendritic tree of an inner NT cell obtained after particle-mediated gene transfer. (*e*) CD15-labeled DB6 axon terminal. (*f*) Merged image showing that the processes of the inner NT cell are closely associated with the axon terminal of the DB6 cell. Panels *a* and *c–f* adapted with permission from Percival et al. (2014). Additional abbreviations: ChAT, choline acetyltransferase; DB, diffuse bipolar; GCL, ganglion cell layer; INL, inner nuclear layer; IPL, inner plexiform layer; LGN, lateral geniculate nucleus.

and ON–OFF responses). The broad thorny cells, however, also differ from local edge detectors in the details of their temporal response properties, which makes them good candidates to detect retinal image slip during smooth pursuit eye movements (Puller et al. 2015). Puller et al. (2015) suggest homology of broad thorny cells to transient ON–OFF ganglion cells reported in the rabbit retina (Sivyer et al. 2011).

5.6. Narrow Thorny Cells

Narrow thorny cells (Dacey et al. 2003) may correspond to the cells named garland cells by Polyak (1941), maze cells by Rodieck & Watanabe (1993), and G8 and G16 cells by Kolb et al. (1992). They have fine nonoverlapping dendrites studded with thorns (**Figure 12*a*,*c***).

5.6.1. Morphology, connectivity with bipolar cells, and molecular markers. The dendrites of the outer narrow thorny cells partially costratify with the outer ChAT bands, whereas the dendrites of inner narrow thorny cells are located below the inner ChAT band, close to the GCL

(Crook et al. 2014b, Masri et al. 2019, Moritoh et al. 2013) (**Figure 12*b***). The inner narrow thorny cells make strong connections with DB6 bipolar cells (Percival et al. 2014) (**Figure 12*d–f***). DB2 and DB3b cells are likely candidates to provide input to the outer narrow thorny cells, but this question has not been investigated specifically. In marmosets, narrow thorny cells express a variety of molecular markers, including calretinin (Chandra et al. 2017) and Satb2 (Nasir-Ahmad et al. 2021), but markers for these cells in macaque and human retinas have yet to be discovered.

5.6.2. Projections and physiology. The brain targets of narrow thorny cells in both macaques and marmosets include the LGN (Dacey et al. 2003, Percival et al. 2014), as well as the superior colliculus (Grünert et al. 2021, Kwan et al. 2019, Rodieck & Watanabe 1993). In marmosets there is some evidence that narrow thorny cells preferentially target koniocellular layer K1 of the LGN (Percival et al. 2014). As the K1 layer contains cells that bypass the primary visual cortex and directly project to the medial temporal cortical area in the brain (Sincich et al. 2004), it can be speculated that narrow thorny cells contribute to residual visual functions (blindsight) that survive damage to the primary visual cortex. To date, however, electrophysiological recordings from narrow thorny ganglion cells are lacking. Similar to the broad thorny cells, the major target of narrow thorny cells is suggested to be the superior colliculus (Masri et al. 2019, Rodieck & Watanabe 1993), but this question has not been studied quantitatively.

5.7. Recursive Cells

Recursive bistratified (RBS) cells have moderately dense dendritic trees that are characterized by small branches curving back toward the soma. Cells with similar morphologies have been classified as part of the T-group of cells in macaques (Rodieck & Watanabe 1993) and the wide-field bistratified cells in humans (Peterson & Dacey 1999, 2000). Based on their morphological resemblance to ON–OFF direction-selective (DS) cells described in the rabbit retina (Vaney et al. 2012), RBS cells were suggested to be involved with direction selectivity (Dacey 2004); this suggestion has been confirmed in preliminary recordings (Detwiler et al. 2019). Like the dendrites of ON–OFF DS cells in rabbits, the dendrites of RBS cells costratify with cholinergic amacrine cells (**Figure 13*b,c***), suggesting that RBS cells make synaptic connections with cholinergic amacrine cells (Crook et al. 2014b, Dacey 2004, Moritoh et al. 2013). The bipolar input may derive from DB2 and DB5 cells, but the exact circuitry of RBS cells in primates has not yet been studied.

RBS (T-group) cells have been found after retrograde tracer injection into the superior colliculus (Dacey 2004, Rodieck & Watanabe 1993), but it cannot be ruled out that they also project to the LGN, as has been found for ON–OFF DS cells in mice (Huberman et al. 2009).

Recursive monostratified cells resemble RBS cells but are monostratified in the ON sublamina (Crook et al. 2014b, Masri et al. 2019). An outer variety has not been found in macaques. In the marmoset retina, an outer recursive monostratified cell has been reported (Moritoh et al. 2013), but the cell shown in their figure 3 resembles an outer smooth monostratified cell. Very little is known about the properties of recursive monostratified cells, but if they are functionally homologous to the ON DS cells in rabbits (Vaney et al. 2012), then they would show ON-type DS responses. Recursive monostratified cells resemble cells in the S-group, which project to the superior colliculus (Rodieck & Watanabe 1993), and they may also target the LGN and the accessory optic system (Dacey 2004).

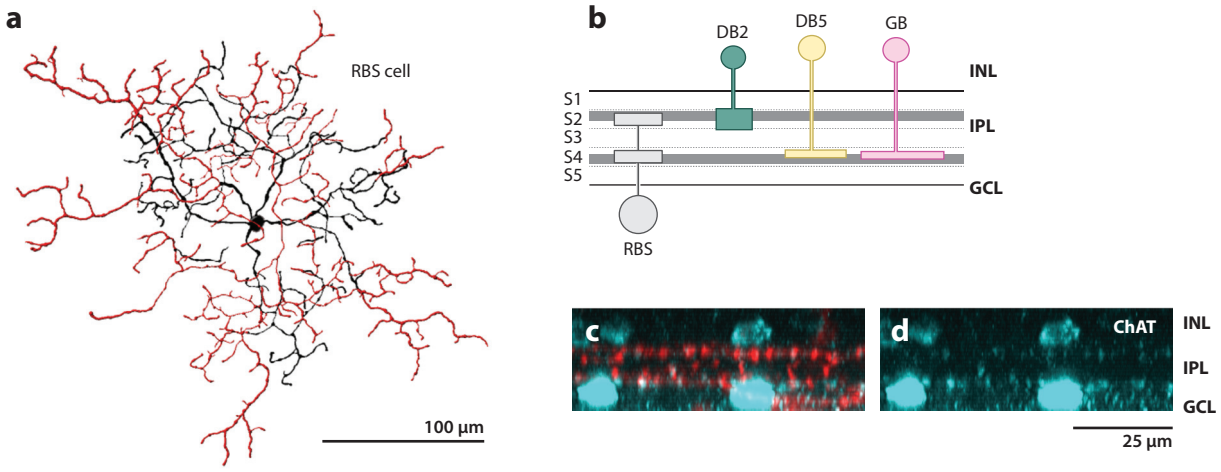

Figure 13

Recursive bistratified (RBS) cells. (*a*) Schematic drawing of an RBS cell from the marmoset retina that was obtained after intracellular DiI injections of Satb1-labeled cells (Lee et al. 2019). The inner dendrites are shown in black, and the outer dendrites are shown in red. Eccentricity is 7 mm. (*b*) Schematic drawing showing costratification of the two dendritic tiers of the RBS cells with the ChAT bands (*gray*) and the suggested bipolar input. (*c*,*d*) Confocal images of the RBS cell shown in panel *a* (orthogonal view). The dendrites of the cell (*red*) are shown with (*c*) ChAT-labeled somas and processes (*cyan*) and (*d*) with ChAT alone. Additional abbreviations: ChAT, choline acetyltransferase; DB, diffuse bipolar; GB, giant bipolar; GCL, ganglion cell layer; INL, inner nuclear layer; IPL, inner plexiform layer.

6. CONCLUSIONS AND FUTURE DIRECTIONS

Setting aside the question of cross-species homology in cell types, similar motifs of connectivity between bipolar and ganglion cells can be identified in the mouse (for a review, see Dunn & Wong 2014) and monkey retina (reviewed above). By this we mean that some bipolar–ganglion cell connections appear to be no stronger than expected by random contacts based on costratification, but others are more selective. In other words, some bipolar and ganglion populations are connected like good friends (e.g., connections between midget bipolar and midget ganglion cells, DB3a and ON parasol cells, and DB6 and narrow thorny inner cells), but other populations make only passing acquaintance. Interestingly, the foveal tight connectivity in the midget pathway is refined from a less specific pattern during foveal development (Zhang et al. 2020).

It is obvious from the estimates of ganglion cell proportions given in **Table 1** that some ganglion cell types may still be missing. However, molecular methods agree with the anatomical estimate of approximately 20 ganglion cell types. Thus, the lower number of ganglion cells in the primate compared to the mouse retina (Baden et al. 2016, Peng et al. 2019) might be a true difference and indicative of the evolutionarily recent specialization of ganglion cells in primates.

What then does the future hold for studies of ganglion cell anatomy and function? The past decade has seen deep and broad advances in molecular analyses and retinal array recordings, and both methods are now firmly established in studies of human and nonhuman primate retinas (for a review, see Picaud et al. 2019). The future, in our view, lies in the potential to combine these approaches with more traditional neuroanatomy, as well as with each other. For example, the field now has 18 fingerprinted ganglion cell molecular clusters, but to date, only a few of them have been assigned to anatomically and physiologically defined cell types. Through the combination of genetic markers with single-cell injection and recording, it is now possible to systematically link the genetic and morphological catalogs. Today, it is not too fanciful to imagine a hybrid molecular-electrode array, where each electrode surface is capable of simultaneously recording

and transfecting a recorded ganglion cell. The future for the study of primate ganglion cells looks bright.

DISCLOSURE STATEMENT

The authors are not aware of any affiliations, memberships, funding, or financial holdings that might be perceived as affecting the objectivity of this review.

ACKNOWLEDGMENTS

We thank our colleagues and students whose work has contributed to many of the studies reviewed here. P. Buzás, A.J. Chandra, K.K. Ghosh, P.R. Jusuf, S.C.S. Lee, R.A. Masri, S. Nasir-Ahmad, K.A. Percival, and B.A. Szmajda made important contributions to this review. We also thank M. Novelli for valuable technical assistance and David W. Marshak for comments on an earlier version of the manuscript.

LITERATURE CITED

Appleby TR, Manookin MB. 2020. Selectivity to approaching motion in retinal inputs to the dorsal visual pathway. *eLife* 9:e51144

Baden T, Berens P, Franke K, Román Rosón M, Bethge M, Euler T. 2016. The functional diversity of retinal ganglion cells in the mouse. *Nature* 529:345–50

Bordt AS, Patterson SS, Girresch RJ, Perez D, Tseng L, et al. 2021. Synaptic inputs to broad thorny ganglion cells in macaque retina. *J. Comp. Neurol.* 529:3098–111

Boycott BB, Wässle H. 1991. Morphological classification of bipolar cells of the primate retina. *Eur. J. Neurosci.* 3:1069–88

Calkins DJ, Schein SJ, Tsukamoto Y, Sterling P. 1994. M and L cones in macaque fovea connect to midget ganglion cells by different numbers of excitatory synapses. *Nature* 371:70–72

Calkins DJ, Sterling P. 2007. Microcircuitry for two types of achromatic ganglion cell in primate fovea. *J. Neurosci.* 27:2646–53

Calkins DJ, Tsukamoto Y, Sterling P. 1998. Microcircuitry and mosaic of a blue-yellow ganglion cell in the primate retina. *J. Neurosci.* 18:3373–85

Chan TL, Martin PR, Clunas N, Grünert U. 2001. Bipolar cell diversity in the primate retina: morphologic and immunocytochemical analysis of a New World monkey, the marmoset *Callithrix jacchus*. *J. Comp. Neurol.* 437:219–39

Chandra AJ, Lee SCS, Grünert U. 2017. Thorny ganglion cells in marmoset retina: morphological and neurochemical characterization with antibodies against calretinin. *J. Comp. Neurol.* 525:3962–74

Chandra AJ, Lee SCS, Grünert U. 2019. Melanopsin and calbindin immunoreactivity in the inner retina of humans and marmosets. *Vis. Neurosci.* 36:E009

Chichilnisky EJ, Baylor DA. 1999. Receptive-field microstructure of blue-yellow ganglion cells in primate retina. *Nat. Neurosci.* 2:889–93

Cowan CS, Renner M, De Gennaro M, Gross-Scherf B, Goldblum D, et al. 2020. Cell types of the human retina and its organoids at single-cell resolution. *Cell* 182:1623–40.e34

Crook JD, Davenport CM, Peterson BB, Packer OS, Detwiler PB, Dacey DM. 2009. Parallel ON and OFF cone bipolar inputs establish spatially-coextensive receptive field structure of blue-yellow ganglion cells in primate retina. *J. Neurosci.* 29:8372–87

Crook JD, Manookin MB, Packer OS, Dacey DM. 2011. Horizontal cell feedback without cone type-selective inhibition mediates "red-green" color opponency in midget ganglion cells of the primate retina. *J. Neurosci.* 31:1762–72

Crook JD, Packer OS, Dacey DM. 2014a. A synaptic signature for ON- and OFF-center parasol ganglion cells of the primate retina. *Vis. Neurosci.* 31:57–84

Crook JD, Packer OS, Troy JB, Dacey DM. 2014b. Synaptic mechanisms of color and luminance coding: rediscovering the X-Y-cell dichotomy in primate retinal ganglion cells. In *The New Visual Neurosciences*, ed. JS Werner, LM Chalupa, pp. 123–43. Cambridge, MA: MIT Press

Crook JD, Peterson BB, Packer OS, Robinson FR, Gamlin PD, et al. 2008a. The smooth monostratified ganglion cell: evidence for spatial diversity in the Y-cell pathway to the lateral geniculate nucleus and superior colliculus in the macaque monkey. *J. Neurosci.* 28:12654–71

Crook JD, Peterson BB, Packer OS, Robinson FR, Troy JB, Dacey DM. 2008b. Y-cell receptive field and collicular projection of parasol ganglion cells in macaque monkey retina. *J. Neurosci.* 28:11277–91

Curcio CA, Allen KA. 1990. Topography of ganglion cells in human retina. *J. Comp. Neurol.* 300:5–25

Curcio CA, Sloan KR, Kalina RE, Hendrickson AE. 1990. Human photoreceptor topography. *J. Comp. Neurol.* 292:497–523

Dacey DM. 1993a. Morphology of a small-field bistratified ganglion cell type in the macaque and human retina. *Vis. Neurosci.* 10:1081–98

Dacey DM. 1993b. The mosaic of midget ganglion cells in the human retina. *J. Neurosci.* 13:5334–55

Dacey DM. 2004. Origins of perception: retinal ganglion cell diversity and the creation of parallel visual pathways. In *The Cognitive Neurosciences*, ed. MS Gazzaniga, pp. 281–301. Cambridge, MA: MIT Press

Dacey DM, Lee BB. 1994. The "blue-on" opponent pathway in primate retina originates from a distinct bistratified ganglion cell type. *Nature* 367:731–35

Dacey DM, Liao H-W, Peterson BB, Robinson FR, Smith VC, et al. 2005. Melanopsin-expressing ganglion cells in primate retina signal colour irradiance and project to the LGN. *Nature* 433:749–54

Dacey DM, Petersen MR. 1992. Dendritic field size and morphology of midget and parasol ganglion cells of the human retina. *PNAS* 89:9666–70

Dacey DM, Peterson BB, Robinson FR, Gamlin PD. 2003. Fireworks in the primate retina: In vitro photodynamics reveals diverse LGN-projecting ganglion cell types. *Neuron* 37:15–27

Detwiler PB, Crook DK, Packer O, Robinson F, Dacey DM. 2019. The recursive bistratified ganglion cell type of the macaque monkey retina is ON-OFF direction selective. *Investig. Ophthalmol. Vis. Sci.* 60:3884

Dhande OS, Stafford BK, Franke K, El-Danaf R, Percival KA, et al. 2019. Molecular fingerprinting of On-Off direction-selective retinal ganglion cells across species and relevance to primate visual circuits. *J. Neurosci.* 39:78–95

Diller L, Packer OS, Verweij J, McMahon MJ, Williams DR, Dacey DM. 2004. L and M cone contributions to the midget and parasol ganglion cell receptive fields of macaque monkey retina. *J. Neurosci.* 24:1079–88

Do MTH. 2019. Melanopsin and the intrinsically photosensitive retinal ganglion cells: biophysics to behavior. *Neuron* 104:205–26

Dunn FA, Wong RO. 2014. Wiring patterns in the mouse retina: collecting evidence across the connectome, physiology and light microscopy. *J. Physiol.* 592:4809–23

Field GD, Chichilnisky EJ. 2007. Information processing in the primate retina: circuitry and coding. *Annu. Rev. Neurosci.* 30:1–30

Field GD, Gauthier JL, Sher A, Greschner M, Machado TA, et al. 2010. Functional connectivity in the retina at the resolution of photoreceptors. *Nature* 467:673–77

Ghosh KK, Goodchild AK, Sefton AE, Martin PR. 1996. Morphology of retinal ganglion cells in a New World monkey, the marmoset *Callithrix jacchus*. *J. Comp. Neurol.* 366:76–92

Ghosh KK, Martin PR, Grünert U. 1997. Morphological analysis of the blue cone pathway in the retina of a New World monkey, the marmoset *Callithrix jacchus*. *J. Comp. Neurol.* 379:211–25

Girresch R. 2020. *Comparative retinal circuitry of parasol and smooth monostratified ganglion cells in macaque central retina*. MA Thesis, St. Louis Univ., MO

Goodchild AK, Martin PR. 1998. The distribution of calcium-binding proteins in the lateral geniculate nucleus and visual cortex of a New World monkey, the marmoset, *Callithrix jacchus*. *Vis. Neurosci.* 15:625–42

Gray DC, Wolfe R, Gee BP, Scoles D, Geng Y, et al. 2008. In vivo imaging of the fine structure of rhodamine-labeled macaque retinal ganglion cells. *Investig. Ophthalmol. Vis. Sci.* 49:467–73

Grünert U, Greferath U, Boycott BB, Wässle H. 1993. Parasol (Pα) ganglion cells of the primate fovea: immunocytochemical staining with antibodies against GABAA receptors. *Vis. Res.* 33:1–14

Grünert U, Jusuf PR, Lee SCS, Nguyen DT. 2011. Bipolar input to melanopsin containing ganglion cells in primate retina. *Vis. Neurosci.* 28:39–50
Grünert U, Lee SCS, Kwan W, Mundinano I, Bourne J, Martin PR. 2021. Retinal ganglion cell types projecting to superior colliculus and pulvinar in marmoset. *Brain Struct. Funct.* In press
Grünert U, Martin PR. 2020. Cell types and cell circuits in human and non human primate retina. *Prog. Retin. Eye Res.* 78:100844
Hannibal J, Christiansen AT, Heegaard S, Fahrenkrug J, Kiilgaard JF. 2017. Melanopsin expressing human retinal ganglion cells: subtypes, distribution, and intraretinal connectivity. *J. Comp. Neurol.* 525:1934–61
Hannibal J, Hindersson P, Østergaard J, Georg B, Heegaard S, et al. 2004. Melanopsin is expressed in PACAP-containing retinal ganglion cells of the human retinohypothalamic tract. *Investig. Ophthalmol. Vis. Sci.* 45:4202–9
Hannibal J, Kankipati L, Strang CE, Peterson BB, Dacey D, Gamlin PD. 2014. Central projections of intrinsically photosensitive retinal ganglion cells in the macaque monkey. *J. Comp. Neurol.* 522:2231–48
Hendrickson A, Yan YH, Erickson A, Possin D, Pow D. 2007. Expression patterns of calretinin, calbindin and parvalbumin and their colocalization in neurons during development of *Macaca* monkey retina. *Exp. Eye Res.* 85:587–601
Hendry SH, Yoshioka T. 1994. A neurochemically distinct third channel in the macaque dorsal lateral geniculate nucleus. *Science* 264:575–77
Hoshino A, Ratnapriya R, Brooks MJ, Chaitankar V, Wilken MS, et al. 2017. Molecular anatomy of the developing human retina. *Dev. Cell* 43:763–79.e4
Huberman AD, Wei W, Elstrott J, Stafford BK, Feller MB, Barres BA. 2009. Genetic identification of an On-Off direction-selective retinal ganglion cell subtype reveals a layer-specific subcortical map of posterior motion. *Neuron* 62:327–34
Hughes TE, Carey RG, Vitorica J, de Blas AL, Karten HJ. 1989. Immunohistochemical localization of GABAA receptors in the retina of the New World primate *Saimiri sciureus*. *Vis. Neurosci.* 2:565–81
Ivanova E, Hwang GS, Pan ZH, Troilo D. 2010. Evaluation of AAV-mediated expression of Chop2-GFP in the marmoset retina. *Investig. Ophthalmol. Vis. Sci.* 51:5288–96
Jacoby RA, Marshak DW. 2000. Synaptic connections of DB3 diffuse bipolar cell axons in macaque retina. *J. Comp. Neurol.* 416:19–29
Jacoby R, Stafford D, Kouyama N, Marshak D. 1996. Synaptic inputs to ON parasol ganglion cells in the primate retina. *J. Neurosci.* 16:8041–46
Jacoby RA, Wiechmann AF, Amara SG, Leighton BH, Marshak DW. 2000. Diffuse bipolar cells provide input to OFF parasol ganglion cells in the macaque retina. *J. Comp. Neurol.* 416:6–18
Jeon C-J, Strettoi E, Masland RH. 1998. The major cell populations of the mouse retina. *J. Neurosci.* 18:8936–46
Johnson JK, Casagrande VA. 1995. Distribution of calcium-binding proteins within the parallel visual pathways of a primate (*Galago crassicaudatus*). *J. Comp. Neurol.* 356:238–60
Jones EG. 2001. The thalamic matrix and thalamocortical synchrony. *Trends Neurosci.* 24:595–601
Joo HR, Peterson BB, Haun TJ, Dacey DM. 2011. Characterization of a novel large-field cone bipolar cell type in the primate retina: evidence for selective cone connections. *Vis. Neurosci.* 28:29–37
Jusuf PR, Lee SCS, Grünert U. 2004. Synaptic connectivity of the diffuse bipolar cell type DB6 in the inner plexiform layer of primate retina. *J. Comp. Neurol.* 469:494–506
Jusuf PR, Lee SCS, Hannibal J, Grünert U. 2007. Characterization and synaptic connectivity of melanopsin-containing ganglion cells in the primate retina. *Eur. J. Neurosci.* 26:2906–21
Jusuf PR, Martin PR, Grünert U. 2006a. Random wiring in the midget pathway of primate retina. *J. Neurosci.* 26:3908–17
Jusuf PR, Martin PR, Grünert U. 2006b. Synaptic connectivity in the midget-parvocellular pathway of primate central retina. *J. Comp. Neurol.* 494:260–74
Jüttner J, Szabo A, Gross-Scherf B, Morikawa RK, Rompani SB, et al. 2019. Targeting neuronal and glial cell types with synthetic promoter AAVs in mice, non-human primates and humans. *Nat. Neurosci.* 22:1345–56

Kaas JH, Huerta MF, Weber JT, Harting JK. 1978. Patterns of retinal terminations and laminar organization of the lateral geniculate nucleus of primates. *J. Comp. Neurol.* 182:517–53

Keenan WT, Rupp AC, Ross RA, Somasundaram P, Hiriyanna S, et al. 2016. A visual circuit uses complementary mechanisms to support transient and sustained pupil constriction. *eLife* 5:e15392

Kling A, Field GD, Brainard DH, Chichilnisky EJ. 2019. Probing computation in the primate visual system at single-cone resolution. *Annu. Rev. Neurosci.* 42:169–86

Kling A, Gogliettino AR, Shah NP, Wu EG, Brackbill N, et al. 2020. Functional organization of midget and parasol ganglion cells in the human retina. bioRxiv 240762. **https://doi.org/10.1101/2020.08.07.240762**

Klug K, Herr S, Tran Ngo I, Sterling P, Schein S. 2003. Macaque retina contains an S-cone OFF midget pathway. *J. Neurosci.* 23:9881–87

Kolb H, DeKorver L. 1991. Midget ganglion cells of the parafovea of the human retina: a study by electron microscopy and serial section reconstructions. *J. Comp. Neurol.* 303:617–36

Kolb H, Linberg KA, Fisher SK. 1992. Neurons of the human retina: a Golgi study. *J. Comp. Neurol.* 318:146–87

Kwan WC, Mundinano IC, de Souza MJ, Lee SCS, Martin PR, et al. 2019. Unravelling the subcortical and retinal circuitry of the primate inferior pulvinar. *J. Comp. Neurol.* 527:558–76

Lee BB, Martin PR, Grünert U. 2010. Retinal connectivity and primate vision. *Prog. Retin. Eye Res.* 29:622–39

Lee BB, Martin PR, Valberg A. 1989. Sensitivity of macaque retinal ganglion cells to chromatic and luminance flicker. *J. Physiol.* 414:223–43

Lee SCS, Martin PR, Grünert U. 2019. Characterization of ganglion cells that express special AT-rich sequence binding protein 1 (SATB1) in primate retina. *Investig. Ophthalmol. Vis. Sci.* 60:5272

Lee SCS, Weltzien F, Madigan MC, Martin PR, Grünert U. 2016. Identification of AII amacrine, displaced amacrine and bistratified ganglion cell types in human retina with antibodies against calretinin. *J. Comp. Neurol.* 524:39–53

Leventhal AG, Rodieck RW, Dreher B. 1981. Retinal ganglion cell classes in the Old World monkey: morphology and central projections. *Science* 213:1139–42

Li PH, Gauthier JL, Schiff M, Sher A, Ahn D, et al. 2015. Anatomical identification of extracellularly recorded cells in large-scale multielectrode recordings. *J. Neurosci.* 35:4663–75

Liao HW, Ren X, Peterson BB, Marshak DW, Yau KW, et al. 2016. Melanopsin-expressing ganglion cells in macaque and human retinas form two morphologically distinct populations. *J. Comp. Neurol.* 524:2845–72

Liu Z, Kurokawa K, Zhang F, Lee JJ, Miller DT. 2017. Imaging and quantifying ganglion cells and other transparent neurons in the living human retina. *PNAS* 114:12803–8

Manookin MB, Patterson SS, Linehan CM. 2018. Neural mechanisms mediating motion sensitivity in parasol ganglion cells of the primate retina. *Neuron* 97:1327–40.e4

Martin PR, Lee BB, White AJR, Solomon SG, Rüttiger L. 2001. Chromatic sensitivity of ganglion cells in the peripheral retina. *Nature* 410:933–36

Martin PR, White AJR, Goodchild AK, Wilder HD, Sefton AE. 1997. Evidence that blue-on cells are part of the third geniculocortical pathway in primates. *Eur. J. Neurosci.* 9:1536–41

Masri RA, Grünert U, Martin PR. 2020. Analysis of parvocellular and magnocellular visual pathways in human retina. *J. Neurosci.* 40:8132–48

Masri RA, Percival KA, Koizumi A, Martin PR, Grünert U. 2016. Connectivity between the OFF bipolar type DB3a and six types of ganglion cell in the marmoset retina. *J. Comp. Neurol.* 524:1839–58

Masri RA, Percival KA, Koizumi A, Martin PR, Grünert U. 2019. Survey of retinal ganglion cell morphology in marmoset. *J. Comp. Neurol.* 527:236–58

McGregor JE, Godat T, Dhakal KR, Parkins K, Strazzeri JM, et al. 2020. Optogenetic restoration of retinal ganglion cell activity in the living primate. *Nat. Commun.* 11:1703

Moritoh S, Komatsu Y, Yamamori T, Koizumi A. 2013. Diversity of retinal ganglion cells identified by transient GFP transfection in organotypic tissue culture of adult marmoset monkey retina. *PLOS ONE* 8:e54667

Nasir-Ahmad S, Lee SCS, Martin PR, Grünert U. 2019. Melanopsin-expressing ganglion cells in human retina: morphology, distribution, and synaptic connections. *J. Comp. Neurol.* 527:312–27

Nasir-Ahmad S, Lee SCS, Martin PR, Grünert U. 2021. Identification of retinal ganglion cell types expressing the transcription factor Satb2 in three primate species. *J. Comp. Neurol.* 529:2727–49
Patterson SS, Bordt AS, Girresch RJ, Linehan CM, Bauss J, et al. 2020a. Wide-field amacrine cell inputs to ON parasol ganglion cells in macaque retina. *J. Comp. Neurol.* 528:1588–98
Patterson SS, Kuchenbecker JA, Anderson JR, Bordt AS, Marshak DW, et al. 2019a. An S-cone circuit for edge detection in the primate retina. *Sci. Rep.* 9:11913
Patterson SS, Kuchenbecker JA, Anderson JR, Neitz M, Neitz J. 2020b. A color vision circuit for non-image-forming vision in the primate retina. *Curr. Biol.* 30:1269–74
Patterson SS, Mazzaferri MA, Bordt AS, Chang J, Neitz M, Neitz J. 2020c. Another blue-ON ganglion cell in the primate retina. *Curr. Biol.* 30:R1409–10
Patterson SS, Neitz M, Neitz J. 2019b. Reconciling color vision models with midget ganglion cell receptive fields. *Front. Neurosci.* 13:865
Peng YR, Shekhar K, Yan W, Herrmann D, Sappington A, et al. 2019. Molecular classification and comparative taxonomics of foveal and peripheral cells in primate retina. *Cell* 176:1222–37
Percival KA, Jusuf PR, Martin PR, Grünert U. 2009. Synaptic inputs onto small bistratified (blue-ON/yellow-OFF) ganglion cells in marmoset retina. *J. Comp. Neurol.* 517:655–69
Percival KA, Koizumi A, Masri RA, Buzás P, Martin PR, Grünert U. 2014. Identification of a pathway from the retina to koniocellular layer K1 in the lateral geniculate nucleus of marmoset. *J. Neurosci.* 34:3821–25
Percival KA, Martin PR, Grünert U. 2011. Synaptic inputs to two types of koniocellular pathway ganglion cells in marmoset retina. *J. Comp. Neurol.* 519:2135–53
Percival KA, Martin PR, Grünert U. 2013. Organisation of koniocellular-projecting ganglion cells and diffuse bipolar cells in the primate fovea. *Eur. J. Neurosci.* 37:1072–86
Perry VH, Cowey A. 1984. Retinal ganglion cells that project to the superior colliculus and pretectum in macaque monkey. *Neuroscience* 12:1125–37
Perry VH, Oehler R, Cowey A. 1984. Retinal ganglion cells that project to the dorsal lateral geniculate nucleus in the macaque monkey. *Neuroscience* 12:1101–23
Peterson BB, Dacey DM. 2000. Morphology of wide-field bistratified and diffuse human retinal ganglion cells. *Vis. Neurosci.* 17:567–78
Peterson BB, Dacey DM. 1999. Morphology of wide-field, monostratified ganglion cells of the human retina. *Vis. Neurosci.* 16:107–20
Petrusca D, Grivich MI, Sher A, Field GD, Gauthier JL, et al. 2007. Identification and characterization of a Y-like primate retinal ganglion cell type. *J. Neurosci.* 27:11019–27
Picaud S, Dalkara D, Marazova K, Goureau O, Roska B, Sahel JA. 2019. The primate model for understanding and restoring vision. *PNAS* 116:26280–87
Polyak SL. 1941. *The Retina*. Chicago: Univ. Chicago Press
Puller C, Manookin MB, Neitz J, Rieke F, Neitz M. 2015. Broad thorny ganglion cells: a candidate for visual pursuit error signaling in the primate retina. *J. Neurosci.* 35:5397–408
Puthussery T, Venkataramani S, Gayet-Primo J, Smith RG, Taylor WR. 2013. NaV1.1 channels in axon initial segments of bipolar cells augment input to magnocellular visual pathways in the primate retina. *J. Neurosci.* 33:16045–59
Reinhard K, Münch TA. 2021. Visual properties of human retinal ganglion cells. *PLOS ONE* 16:e0246952
Rhoades CE, Shah NP, Manookin MB, Brackbill N, Kling A, et al. 2019. Unusual physiological properties of smooth monostratified ganglion cell types in primate retina. *Neuron* 103:658–72.e6
Rockhill RL, Daly FJ, MacNeil MA, Brown SP, Masland RH. 2002. The diversity of ganglion cells in a mammalian retina. *J. Neurosci.* 22:3831–43
Rodieck RW. 1991. Which cells code for color? In *From Pigments to Perception: Advances in Understanding Visual Processes*, ed. A Valberg, BB Lee, pp. 83–93. New York: Plenum Press
Rodieck RW, Watanabe M. 1993. Survey of the morphology of macaque retinal ganglion cells that project to the pretectum, superior colliculus, and parvocellular laminae of the lateral geniculate nucleus. *J. Comp. Neurol.* 338:289–303
Roy S, Jayakumar J, Martin PR, Dreher B, Saalmann YB, et al. 2009. Segregation of short-wavelength-sensitive (S) cone signals in the macaque dorsal lateral geniculate nucleus. *Eur. J. Neurosci.* 30:1517–26

Schein SJ. 1988. Anatomy of macaque fovea and spatial densities of neurons in foveal representation. *J. Comp. Neurol.* 269:479–505

Silveira LC, Lee BB, Yamada ES, Kremers J, Hunt DM, et al. 1999. Ganglion cells of a short wavelength sensitive cone pathway in New World monkeys: morphology and physiology. *Vis. Neurosci.* 16:333–43

Silveira LC, Perry VH. 1991. The topography of magnocellular projecting ganglion cells (M-ganglion cells) in the primate retina. *Neuroscience* 40:217–37

Silveira LC, Saito CA, Lee BB, Kremers J, da Silva Filho M, et al. 2004. Morphology and physiology of primate M- and P-cells. *Prog. Brain Res.* 144:21–46

Sincich LC, Park KF, Wohlgemuth MJ, Horton JC. 2004. Bypassing V1: a direct geniculate input to area MT. *Nat. Neurosci.* 7:1123–28

Sinha R, Hoon M, Baudin J, Okawa H, Wong RO, Rieke F. 2017. Cellular and circuit mechanisms shaping the perceptual properties of the primate fovea. *Cell* 168:413–26.e12

Sivyer B, Venkataramani S, Taylor WR, Vaney DI. 2011. A novel type of complex ganglion cell in rabbit retina. *J. Comp. Neurol.* 519:3128–38

Solomon SG, Martin PR, White AJR, Rüttiger L, Lee BB. 2002. Modulation sensitivity of ganglion cells in peripheral retina of macaque. *Vis. Res.* 42:2893–98

Soto F, Hsiang JC, Rajagopal R, Piggott K, Harocopos GJ, et al. 2020. Efficient coding by midget and parasol ganglion cells in the human retina. *Neuron* 107:656–66

Sweeney NT, James KN, Nistorica A, Lorig-Roach RM, Feldheim DA. 2019. Expression of transcription factors divides retinal ganglion cells into distinct classes. *J. Comp. Neurol.* 527:225–35

Szmajda BA, Buzás P, FitzGibbon T, Martin PR. 2006. Geniculocortical relay of blue-off signals in the primate visual system. *PNAS* 103:19512–17

Szmajda BA, Grünert U, Martin PR. 2008. Retinal ganglion cell inputs to the koniocellular pathway. *J. Comp. Neurol.* 510:251–68

Telkes I, Lee SC, Jusuf PR, Grünert U. 2008. The midget-parvocellular pathway of marmoset retina: a quantitative light microscopic study. *J. Comp. Neurol.* 510:539–49

Thoreson WB, Dacey DM. 2019. Diverse cell types, circuits, and mechanisms for color vision in the vertebrate retina. *Physiol. Rev.* 99:1527–73

Tsukamoto Y, Omi N. 2015. OFF bipolar cells in macaque retina: type-specific connectivity in the outer and inner synaptic layers. *Front. Neuroanat.* 9:122

Tsukamoto Y, Omi N. 2016. ON bipolar cells in macaque retina: type-specific synaptic connectivity with special reference to OFF counterparts. *Front. Neuroanat.* 10:104

Turner MH, Rieke F. 2016. Synaptic rectification controls nonlinear spatial integration of natural visual inputs. *Neuron* 90:1257–71

van Wyk M, Taylor WR, Vaney DI. 2006. Local edge detectors: a substrate for fine spatial vision at low temporal frequencies in rabbit retina. *J. Neurosci.* 26:13250–63

Vaney DI. 1980. A quantitative comparison between the ganglion cell populations and axonal outflows of the visual streak and periphery of the rabbit retina. *J. Comp. Neurol.* 189:215–33

Vaney DI, Sivyer B, Taylor WR. 2012. Direction selectivity in the retina: symmetry and asymmetry in structure and function. *Nat. Rev. Neurosci.* 13:194–208

Wässle H. 2004. Parallel processing in the mammalian retina. *Nat. Rev. Neurosci.* 5:747–57

Wässle H, Grünert U, Martin PR, Boycott BB. 1994. Immunocytochemical characterization and spatial distribution of midget bipolar cells in the macaque monkey retina. *Vis. Res.* 34:561–79

Wässle H, Grünert U, Röhrenbeck J, Boycott BB. 1989. Cortical magnification factor and the ganglion cell density of the primate retina. *Nature* 341:643–46

Wässle H, Peichl L, Boycott BB. 1981. Dendritic territories of cat retinal ganglion cells. *Nature* 292:344–45

Watanabe M, Rodieck RW. 1989. Parasol and midget ganglion cells of the primate retina. *J. Comp. Neurol.* 289:434–54

Weltzien F, Percival KA, Martin PR, Grünert U. 2015. Analysis of bipolar and amacrine populations in marmoset retina. *J. Comp. Neurol.* 523:313–34

Wilder HD, Grünert U, Lee BB, Martin PR. 1996. Topography of ganglion cells and photoreceptors in the retina of a New World monkey: the marmoset *Callithrix jacchus*. *Vis. Neurosci.* 13:335–52

Wool LE, Crook JD, Troy JB, Packer OS, Zaidi Q, Dacey DM. 2018. Nonselective wiring accounts for red-green opponency in midget ganglion cells of the primate retina. *J. Neurosci.* 39:1520–40

Wool LE, Packer OS, Zaidi Q, Dacey DM. 2019. Connectomic identification and three-dimensional color tuning of S-OFF midget ganglion cells in the primate retina. *J. Neurosci.* 39:7893–909

Yamada ES, Bordt AS, Marshak DW. 2005. Wide-field ganglion cells in macaque retinas. *Vis. Neurosci.* 22:383–93

Yamada ES, Marshak DW, Silveira LCL, Casagrande VA. 1998. Morphology of P and M retinal ganglion cells of the bush baby. *Vis. Res.* 38:3345–52

Yan W, Peng YR, van Zyl T, Regev A, Shekhar K, et al. 2020. Cell atlas of the human fovea and peripheral retina. *Sci. Rep.* 10:9802

Yin L, Greenberg K, Hunter JJ, Dalkara D, Kolstad KD, et al. 2011. Intravitreal injection of AAV2 transduces macaque inner retina. *Investig. Ophthalmol. Vis. Sci.* 52:2775–83

Yin L, Masella B, Dalkara D, Zhang J, Flannery JG, et al. 2014. Imaging light responses of foveal ganglion cells in the living macaque eye. *J. Neurosci.* 34:6596–605

Zhang C, Kim YJ, Silverstein AR, Hoshino A, Reh TA, et al. 2020. Circuit reorganization shapes the developing human foveal midget connectome toward single-cone resolution. *Neuron* 108:P906–18.E3